A Genetic Network for Systemic RNA Silencing in Plants[1] [OPEN]

Weiwei Chen,[a,2] Xian Zhang,[a,2] Yaya Fan,[a,2] Bin Li,[a,2] Eugene Ryabov,[a,b,2] Nongnong Shi,[a] Mei Zhao,[a] Zhiming Yu,[a] Cheng Qin,[a] Qianqian Zheng,[a] Pengcheng Zhang,[a] Huizhong Wang,[a] Stephen Jackson,[b] Qi Cheng,[c] Yule Liu,[d] Philippe Gallusci,[e] and Yiguo Hong[a,b,f,3]

[a]Research Centre for Plant RNA Signaling, College of Life and Environmental Sciences, Hangzhou Normal University, Hangzhou 310036, China
[b]Warwick-Hangzhou RNA Signaling Joint Laboratory, School of Life Sciences, University of Warwick, Warwick CV4 7AL, United Kingdom
[c]Biotechnology Research Institute, Chinese Academy of Agricultural Sciences, Beijing 100081, China
[d]Centre for Plant Biology and MOE Key Laboratory of Bioinformatics, School of Life Sciences, Tsinghua University, Beijing 100084, China
[e]UMR EGFV, Bordeaux Sciences Agro, INRA, Université de Bordeaux, 210 Chemin de Leysotte, CS 50008, 33882 Villenave d'Ornon, France
[f]Worcester-Hangzhou Joint Molecular Plant Health Laboratory, Institute of Science and the Environment, University of Worcester, WR2 6AJ, United Kingdom

ORCID IDs: 0000-0002-4265-9714 (E.R.); 0000-0001-5406-9749 (Z.Y.); 0000-0002-4423-6045 (Y.L.); 0000-0003-1163-8299 (P.G.); 0000-0002-3352-9686 (Y.H.).

Non-cell autonomous RNA silencing can spread from cell to cell and over long distances in animals and plants. However, the genetic requirements and signals involved in plant mobile gene silencing are poorly understood. Here, we identified a *DICER-LIKE2* (*DCL2*)-dependent mechanism for systemic spread of posttranscriptional RNA silencing, also known as posttranscriptional gene silencing (PTGS), in *Nicotiana benthamiana*. Using a suite of transgenic *DCL* RNAi lines coupled with a GFP reporter, we demonstrated that *N. benthamiana* DCL1, DCL2, DCL3, and DCL4 are required to produce microRNAs and 22, 24, and 21nt small interfering RNAs (siRNAs), respectively. All investigated siRNAs produced in local incipient cells were present at low levels in distal tissues. Inhibition of *DCL2* expression reduced the spread of gene silencing, while suppression of *DCL3* or *DCL4* expression enhanced systemic PTGS. In contrast to *DCL4* RNAi lines, *DCL2-DCL4* double-RNAi lines developed systemic PTGS similar to that observed in *DCL2* RNAi. We further showed that the 21 or 24 nt local siRNAs produced by DCL4 or DCL3 were not involved in long-distance gene silencing. Grafting experiments demonstrated that *DCL2* was required in the scion to respond to the signal, but not in the rootstock to produce/send the signal. These results suggest a coordinated *DCL* genetic pathway in which *DCL2* plays an essential role in systemic PTGS in *N. benthamiana*, while both *DCL4* and *DCL3* attenuate systemic PTGS. We discuss the potential role of 21, 22, and 24 nt siRNAs in systemic PTGS.

RNA silencing is a cellular gene regulatory mechanism that is conserved across fungal, plant, and animal kingdoms (Baulcombe, 2004; Sarkies and Miska, 2014). Through sequence-specific targeting, RNA silencing can degrade mRNA for posttranscriptional gene silencing (PTGS) or modify related DNA for transcriptional gene silencing (TGS). In plants, primary silencing is triggered by double-stranded RNA (dsRNA) molecules, which are processed into 21 to 24 nucleotide (nt) small-interfering (si) RNA duplexes, known as primary siRNAs, by *DICER-LIKE* (*DCL*) RNase III-like enzymes (Baulcombe, 2004; Sarkies and Miska, 2014). For instance, dsRNA can be directly produced from a hairpin transgene in primary silencing (Mlotshwa et al., 2008). Primary silencing differs from transitive silencing, in which the trigger is initially not itself dsRNA. In contrast to primary silencing, the dsRNA in transitive silencing is produced from a single-stranded (ss) RNA template, and requires the coordinated activity of a set of genes. These genes include *DCL2*, *RNA dependent RNA polymerase 6* (*RDR6*), and *SGS3*, the latter of which encodes a coiled-coiled domain protein (Mlotshwa et al., 2008; Parent et al., 2015). Transitive silencing cascades and amplifies cell and non-cell autonomous silencing to other parts of the target RNA, leading to generation of secondary siRNAs. It is well known that *DCL2* plays an essential role in cell-autonomous silencing transitivity and accumulation of secondary siRNAs in Arabidopsis (*Arabidopsis thaliana*; Mlotshwa et al., 2008; Parent et al., 2015).

In animals and plants, TGS and PTGS can spread from cell to cell, systemically, or even between different organisms (Weiberg et al., 2013). Intercellular and long-distance movement of non-cell autonomous RNA silencing involves mobile signals and various genetic components (Melnyk et al., 2011b; Molnar et al., 2010). For example, SNF2, a JmjC domain protein JMJ14, the

THO/TREX mRNA export complex, and RDR6 are all associated with intercellular RNA silencing (Qin et al., 2012; Searle et al., 2010; Smith et al., 2007; Yelina et al., 2010). Moreover, RDR6 also contributes to initial signal perception for systemic PTGS (Melnyk et al., 2011b). Intriguingly, *NRPD1a*, encoding RNA polymerase IVa, *RDR2*, and *DCL3*, which all function in a chromatin silencing pathway, are required for the reception of long-distance mRNA PTGS, and Argonaute4 is also partially involved in the reception of such long-distance silencing. *DCL4* and *DCL2* then act hierarchically, as they do in antiviral resistance, to produce 21 and 22 nt siRNAs, respectively, which guide mRNA degradation in systemic tissues (Brosan et al., 2007).

Arabidopsis, and most likely other plant species, possess four DCL RNase III family enzymes for small RNA (sRNA) biogenesis. DCL1 is involved in microRNA (miRNA) production and DCL2, DCL3, and DCL4 are involved in 22, 24, and 21 nt siRNA production, respectively (Henderson et al., 2006; Mukherjee et al., 2013; Xie et al., 2004). DCL1-generated miRNAs can move and act as local and distal signals that play essential roles in plant growth and development, although direct evidence for mobile miRNA signaling is lacking (Carlsbecker et al., 2010; Pant et al., 2008; Skopelitis et al., 2017). The DCL3-processed 24 nt siRNA has been shown to direct systemic TGS that controls genome-wide DNA methylation in recipient cells through RNA-directed DNA methylation of homologous genomic DNA sequences (Henderson et al., 2006; Lewsey et al., 2016; Melnyk et al., 2011a; Molnar et al., 2010; Sarkies and Miska, 2014). However, systemic silencing has also been reported to occur in the absence of sRNAs (Mallory et al., 2001), and no specific siRNAs produced by any of the four DCLs were found to be associated with systemic silencing (Brosnan et al., 2007). Moreover, even in Arabidopsis, different genetic factors required for mobile PTGS have been discovered from mutant screens in very similar experimental systems (Melnyk et al., 2011b). Thus, the precise nature of long-distance mobile signal remains to be elucidated, as this signal is not exclusively produced by any of the four DCLs. Crucial molecular events during systemic RNA silencing reception were elegantly investigated in Arabidopsis (Brosnan et al., 2007). Nevertheless, these findings contrast with systemic silencing, known as RNA interference (RNAi) in animals, where the mobile signal is dsRNA (Jose et al., 2011). In *Caenorhabditis elegans*, systemic RNAi involves intertissue transfer and entry of gene-specific dsRNAs into the cytosol by the dsRNA-selective importer SID-1 (Winston et al., 2002; Feinberg and Hunter, 2003; Shih and Hunter, 2011). Consequently, mobile dsRNAs expressed in a variety of somatic tissues can lead to SID-1-dependent homologous RNAi of target mRNA in other somatic tissues, or even transgenerational silencing (Jose et al., 2009; Devanapally et al., 2015).

The intricate functions of *DCL2* and *DCL4* are partially redundant in trans-acting siRNA biogenesis and in plant antiviral defense. However, DCL2 is responsible for 22 nt siRNA biosynthesis and has different roles to DCL4 in the production of primary and secondary siRNAs (Chen et al., 2010; Henderson et al., 2006; Qu et al., 2008; Wang et al., 2011; Xie et al., 2005). DCL4-processed 21nt siRNA is mainly involved in intracellular PTGS as well as represents the signaling molecule that moves from leaf companion cells to adjacent cells to induce limited intercellular PTGS in Arabidopsis (Dunoyer et al., 2005). Interestingly, *DCL2* expression in leaf vascular tissues enhances PTGS in surrounding cells in Arabidopsis. DCL2 is thought to promote the production of 22 nt siRNAs that then stimulate 21 nt siRNA biogenesis via RDR6 and DCL4, resulting in increased cell-to-cell spread of PTGS (Parent et al., 2015). By contrast, *DCL4* inhibits the cell-to-cell spread of virus-induced gene silencing (VIGS), a form of PTGS, while *DCL2*, likely along with a DCL2-dependent RNA signal, is required for efficient trafficking of VIGS from epidermal to adjacent cells (Qin et al., 2017). However, the roles of 21 and 24 nt siRNAs and other types of RNA molecules in mobile PTGS and TGS are under debate (Mallory et al., 2001; Brosnan et al., 2007; Melnyk et al., 2011b; Sarkies and Miska, 2014) and remain highly controversial (Berg, 2016).

On the other hand, impairment of *DCL2* or *DCL4* can reduce or promote cell-autonomous PTGS, and *DCL2* promotes intracellular transitive silencing in Arabidopsis (Mlotshwa et al., 2008; Parent et al., 2015). Moreover, two different strong viral suppressors of silencing (*Turnip crinkle virus* P38 and *Turnip mosaic virus* HC-Pro) block the accumulation of secondary siRNAs produced by transitive silencing (Mlotshwa et al., 2008). Thus, *DCL2* may have a role in viral defense that can be coupled to intercellular and systemic PTGS. This view is indeed supported by the requirement of *DCL2* and DCL2-dependent mobile signals for intercellular antiviral silencing in *N. benthamiana* (Qin et al., 2017). A genetic screen for impaired systemic RNAi revealed that *DCL2* is crucial for *RDR6*-dependent systemic

[1] This work was supported by grants from the National Natural Science Foundation of China (NSFC 31370180 to Y.H.); Ministry of Agriculture of the People's Republic of China (the National Transgenic Program of China 2016ZX08009001-004 to Y.H.); Ministry of Science and Technology of the People's Republic of China (2017YFE0110900 to Y.H.); Hangzhou Normal University (Pandeng Program 201108 to Y.H.); the Hangzhou City Government (Innovative Program for Science Excellence 20131028 to Y.H.); NSFC (31601765 to W.C., 31201490 to X.Z., 31500251 to C.Q.); Zhejiang Provincial Natural Science Foundation (LY15C140006 to X.Z., LY14C010005 to N.S.); and the UK Biotechnology and Biological Sciences Research Council (UK-China Partnering Award BB/K021079/1 to S.J. and Y.H.).

[2] These authors contributed equally to this work.

[3] Address correspondence to yiguo.hong@hznu.edu.cn, yiguo.hong@warwick.ac.uk, and y.hong@worc.ac.uk. .

The author responsible for distribution of materials integral to the findings presented in this article in accordance with the policy described in the instructions for Authors (www.plantphysioll.org) is: Yiguo Hong (yiguo.hong@hznu.edu.cn, yiguo.hong@warwick.ac.uk, and y.hong@worc.ac.uk).

[OPEN] Articles can be viewed without a subscription.
www.plantphysiol.org/cgi/doi/10.1104/pp.17.01828

Table I. Summary of transgenic lines generated and used in this study

Wild-Type and Transgenic Lines	Genetic Background and Cross	Transgene Information
Nb	*N. benthamiana*	Wild-type, no transgene
DCL1i	RNAi of *DCL1* in *Nb*	pRNAi-DCL1, single copy, hemizygous
DCL2Ai	RNAi of *DCL2* in *Nb*	pRNAi-DCL2, single copy, homozygous
DCL2Bi		
DCL3Ai	RNAi of *DCL3* in *Nb*	pRNAi-DCL3, single copy, homozygous
DCL3Bi		
DCL4Ai	RNAi of *DCL4* in *Nb*	pRNAi-DCL4, single copy, homozygous
DCL4Bi		
RDR6i (Gift from David Baulcombe)	RNAi of *NbRDR6* in *Nb*	*RDR6* hairpin, single copy, homozygous
DCL24i	Cross between *DCL2Ai* and *DCL4Bi*	pRNAi-DCL2, single copy, hemizygous pRNAi-DCL4, single copy, hemizygous
16cGFP	GFP transgenic line in *Nb*	35S-GFP, single copy, homozygous
GfpRDR6i (Gift from David Baulcombe)	RNAi of *RDR6* in *16cGFP*	35S-GFP, single copy, homozygous *RDR6* hairpin, single copy, homozygous
GfpDCL1i	RNAi of *DCL1* in *16cGFP*	35S-GFP, single copy, homozygous pRNAi-DCL1, single copy, hemizygous
GfpDCL2Ai	Cross between *16cGFP* and *DCL2Ai*	35S-GFP, single copy, hemizygous
GfpDCL2Bi	Cross between *16cGFP* and *DCL2Bi*	pRNAi-DCL2, single copy, hemizygous
GfpDCL3Ai	Cross between *16cGFP* and *DCL3Ai*	35S-GFP, single copy, hemizygous
GfpDCL3Bi	Cross between *16cGFP* and *DCL3Bi*	pRNAi-DCL3, single copy, hemizygous
GfpDCL4Ai	Cross between *16cGFP* and *DCL4Ai*	35S-GFP, single copy, hemizygous
GfpDCL4Bi	Cross between *16cGFP* and *DCL4Bi*	pRNAi-DCL4, single copy, hemizygous
GfpDCL24Ai	Triple cross among *16c, DCL2Ai* and *DCL4Ai*	35S-GFP, single copy, hemizygous
GfpDCL24Bi	Triple cross among *16c, DCL2Ai* and *DCL4Bi*	pRNAi-DCL2, single copy, hemizygous pRNAi-DCL4, single copy, hemizygous
homGfpDCL2Ai	Self from *GfpDCL2Ai*	35S-GFP, single copy, homozygous pRNAi-DCL2, single copy, homozygous
homGfpDCL3Bi	Self from *GfpDCL3Bi*	35S-GFP, single copy, homozygous pRNAi-DCL3, single copy, homozygous
homGfpDCL4Ai	Self from *GfpDCL4Ai*	35S-GFP, single copy, homozygous pRNAi-DCL4, single copy, homozygous
GfpDCL24Ci	Cross between *homGfpDCL2Ai* and *homGfpDCL4Ai*	35S-GFP, single copy, homozygous pRNAi-DCL2, single copy, hemizygous pRNAi-DCL4, single copy, hemizygous
Gfp	Cross between *Nb* and *16cGFP*	35S-GFP, single copy, hemizygous

PTGS (Taochy et al., 2017). Nevertheless, it is not known whether, and to what extent, *DCL2* and other *DCLs* regulate systemic silencing. However, DCL2 and its cognate 22 nt siRNA are clearly able to affect secondary siRNA biogenesis, antiviral defense, and plant development (Bouché et al., 2006; Chen et al. 2010; Garcia-Ruiz et al., 2010; Qin et al., 2017; Wang et al., 2011).

In this article, we report the genetic requirement of a *DCL* network and the involvement of mobile siRNAs in the systemic spread of PTGS in *N. benthamiana.*

RESULTS

Genetic Resources for Examining Mobile RNA Silencing in *N. benthamiana*

To investigate systemic RNA silencing in *N. benthamiana*, we used gene-specific RNAi to inhibit the four *DCLs* orthologous to Arabidopsis *DCL1*, *DCL2*, *DCL3*, and *DCL4* (Supplemental Data Set S1). Specific genes or gene fragments were PCR-amplified and cloned into the overexpression vector pCAMBIA1300 to produce p35S-GFP_{714} (the GFP coding sequence of this variant is 714 nt long; Ryabov et al., 2004) or the hairpin RNAi vector pRNAi-LIC (Xu et al., 2010) to generate pRNAi-GFP_{714} and pRNAi-DCLs (Supplemental Fig. S1). These cloned *DCL* gene fragments shared no detectable nucleotide sequence similarity (Supplemental Table S1). Plants were then transformed with each of the pRNAi-DCL constructs. We selected two single-copy homozygous RNAi lines, *DCL2Ai* and *DCL2Bi* for *DCL2*, *DCL3Ai* and *DCL3Bi* for *DCL3*, and *DCL4Ai* and *DCL4Bi* for *DCL4*, and produced a double RNAi line *DCL24i* through crossing *DCL2Ai* with *DCL4Bi* (Table I). We crossed all of the individual *DCL* RNAi lines with the *16cGFP* plants bearing a single copy of a *GFP* transgene (referred to as GFP_{792}, as the coding region of this gene variant is 792 nt long) under the control of the 35S promoter (Haseloff et al., 1997; Ruiz et al., 1998) to create the hybrid lines *Gfp*, *GfpDCL2Ai*, *GfpDCL2Bi*, *GfpDCL3Ai*, *GfpDCL3Bi*, *GfpDCL4Ai*, *GfpDCL4Bi*, *GfpDCL24Ai*, and *GfpDCL24Bi* (Table I). Through selfing, we generated homozygous lines *homGfpDCL2Ai*, *homGfpDCL3Bi*, and *homGfpDCL4Ai*. An additional double *DCL2-DCL4* RNAi line *GfpDCL24Ci* was obtained through crossing *homGfpDCL2Ai* and *homGfpDCL4Ai* (Table I). However,

we only obtained one hemizygous *DCL1i* or *GfpDCL1i* line by transforming *N. benthamiana* or *16cGFP* with pRNAi-DCL1, as homozygous *DCL1* RNAi was lethal (Table I). Lines *RDR6i* and *GfpRDR6i* were included in this work (Schwach et al., 2005). To confirm the inhibition caused by RNAi, we performed RT-qPCR and analyzed *DCL* mRNA levels in the RNAi lines. Gene-specific RNAi repression of *DCL2*, *DCL3*, and *DCL4* was between 70% and 90%, and approximately 45% suppression was achieved for *DCL1* (Supplemental Fig. S2), consistent with our previous analyses (Qin et al., 2017).

DCLs Function Differentially to Generate Small RNAs in *N. benthamiana*

To determine whether individual *DCLs* function differently to generate 21, 22, and 24 nt siRNAs in *N. benthamiana* (Fig. 1), we used a GFP reporter system and performed a local PTGS assay (Ruiz et al., 1998; Ryabov et al., 2004). Leaves of the *DCL* RNAi plants at the six-leaf stage were co-infiltrated with *Agrobacterium* harboring p35-GFP$_{714}$ and *Agrobacterium* harboring pRNAi-GFP$_{714}$ or an empty pRNAi-LIC vector (Supplemental Figs. S1 and S3A). Compared to the non-RNAi wild-type plant (Fig. 1A), RNAi of *DCL1* (*DCL1i*; Fig. 1B), *DCL2* (DCL2Ai and DCL2Bi; Fig. 1, C and D), and *DCL3* (DCL3Ai and DCL3Bi; Fig. 1, E and F) did not affect local RNA silencing, but RNAi of *DCL4* (DCL4Ai, DCL4Bi, and DCL24i; Fig. 1, G–I) weakened local PTGS. This is evident by almost complete (Fig. 1, A–F, left) or partial reduction (Fig. 1, G–I, left) in GFP fluorescence intensity in the coagroinfiltrated lamina (Supplemental Fig. S4). Consistent with the level of RNAi achieved, only a low level of *GFP$_{714}$* mRNA was detected in wild-type, *DCL2Ai*, *DCL2Bi*, *DCL3Ai*, and *DCL3Bi* plants, whereas a relatively high level of *GFP$_{714}$* mRNA was found in *DCL4Ai*, *DCL4Bi*, and *DCL24i* plants (Fig. 1J). We also noticed that the *GFP$_{714}$* mRNA levels were slightly higher in *DCL1i* plants (Fig. 1J).

We then used northern hybridizations to characterize siRNAs present in the infiltrated leaf tissues of different *DCL* RNAi lines (Fig. 1K). These local siRNAs are hereafter designated L-siRNAs. L-siRNAs include primary siRNAs that are directly generated from the hairpin *GFP$_{714}$* dsRNA and secondary siRNAs that are generated from the p35S-GFP$_{714}$ expressed *GFP$_{714}$* mRNA. There is some variation in the levels of siRNAs detected in the two independent RNAi lines with respect to a given *DCL* gene. Nevertheless, 21, 22, and 24 nt L-siRNAs were readily detectable in the control and *DCL1i* plants. This contrasted with the specific loss of 22 nt L-siRNAs in *DCL2Ai* and *DCL2Bi*, 24 nt L-siRNAs in *DCL3Ai* and *DCL3Bi*, and 21 nt L-siRNAs in *DCL4Ai* and *DCL4Bi* (Fig. 1K). We also noticed a large amount of 22 and 24 nt L-siRNAs in *DCL4Ai* and *DCL4Ai*, and a high level of 24 nt L-siRNAs in *DCL2Ai* and *DCL2Bi*. However, 21 and 22 nt L-siRNAs were undetectable in the *DCL24i* plants (Fig. 1K). These data reveal that in *N. benthamiana*, as in Arabidopsis, DCL4, DCL2, and DCL3 are required to produce 21, 22, and 24 nt siRNAs, respectively.

RNAseq Analysis Confirms *DCLs* for Biosynthesis of sRNAs in *N. benthamiana*

To further investigate how *DCL* RNAi affects sRNA synthesis, we collected agro-infiltrated leaf tissues from *N. benthamiana* (*Nb*), *DCL1i*, *DCL2Ai*, *DCL2Bi*, *DCL3Ai*, *DCL3Bi*, *DCL4Ai*, *DCL4Bi*, and *RDR6i* plants at 7 d post agro-infiltration (dpa). The leaves were co-infiltrated with agrobacterium harboring p35S-GFP$_{714}$ and agrobacterium harboring pRNAi-GFP$_{714}$ (Fig. 2; Supplemental Fig. S3A). We then constructed 9 individual local sRNA libraries for next generation sequencing (NGS) and generated approximately 11 million sRNA reads for each library (Supplemental Table S2). We found that (1) gene-specific RNAi of *DCLs* or *RDR6* had no off-target effect on other silencing-related genes (Supplemental Fig. S5); (2) correlation analyses of total miRNAs among these sRNA libraries validated the authenticity and direct comparability of the detected sRNA profiles (Supplemental Tables S3 and S4); and (3) *DCL1* RNAi resulted in a clear reduction of miRNAs (Supplemental Fig. S6; Supplemental Table S2). Compared to *Nb*, *DCL1i*, and *RDR6i* (Fig. 2, A, B, and I, left), decreased levels in 21, 22, and 24 nt *GFP$_{714}$* L-siRNAs and total sRNAs correlated with RNAi of *DCL4*, *DCL2*, and *DCL3* (Fig. 2, C–H, left; Supplemental Fig. S3, B–J). These data are consistent with the sRNA northern detection (Fig. 1K) and further show that as in Arabidopsis, DCL1 is also required for miRNA biosynthesis in *N. benthamiana*.

Detection of L-siRNAs in Distal Systemic Leaves

To investigate whether *GFP$_{714}$* L-siRNAs generated in local leaves are able to move systemically to distant tissues (Fig. 3), we collected a pool of young systemic leaves from the agro-infiltrated *DCL* RNAi or control plants at 14 dpa and constructed 9 systemic leaf sRNA libraries for NGS (Supplemental Fig. S3A). Similar to the local sRNA libraries made from the infiltrated leaf tissues, we generated approximately 11 million sRNA reads for each of the systemic libraries, and *DCL*-specific RNAi was again found to have little off-target effect on other silencing-related genes in the systemic leaves (Supplemental Table S2; Supplemental Fig. S5). We then scrutinized the systemic leaf sRNA datasets for reads matching the *GFP$_{714}$* mRNA. Different levels of both sense and antisense 21, 22, and 24 nt *GFP$_{714}$* L-siRNAs were detected in systemic leaves of *Nb*, *RDR6i*, and *DCL* RNAi plants (Fig. 2, A–I, right), although the total number of *GFP$_{714}$* L-siRNA (and total sRNA) reads in the infiltrated leaves was similar among all samples (Fig. 2, A–I, left; Supplemental Table S2). We detected high levels of 22 nt L-siRNAs, some 21 nt L-siRNAs, and a low level of 24 nt L-siRNAs in systemic *Nb* leaves (Fig. 2A, right). However, in the young leaves of *DCL1i*, *DCL2Ai*, *DCL2Bi*, and *RDR6i* plants (Fig. 2, B–D and I, right), the number of 22 or 21 nt L-siRNA

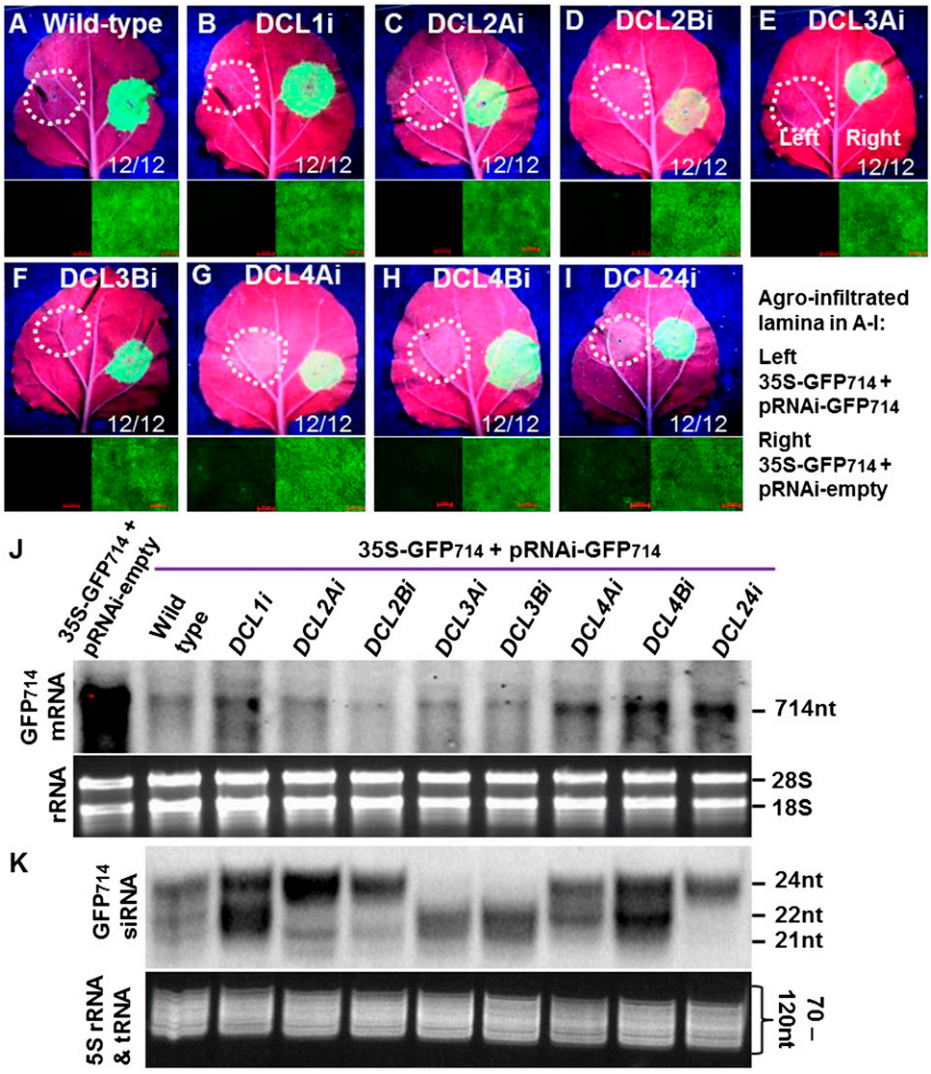

Figure 1. Impact of *DCL* RNAi on local hairpin dsRNA-mediated PTGS. A to I, Local PTGS assay. The left half of leaves of *N. benthamiana* (A), *DCL1i* (B), *DCL2Ai* and *DCL2Bi* (C and D), *DCL3Ai* and *DCL3Bi* (E and F), *DCL4Ai* and *DCL4Bi* (G and H), and *DCL24i* (I) plants were co-infiltrated with agrobacterium harboring p35S-GFP_{714} and pRNAi-GFP_{714} and the right half with p35S-GFP_{714} and the pRNAi-empty vector. Without PTGS, GFP_{714} expression from p35S-GFP_{714} shows strong green fluorescence. Induction of PTGS by the hairpin GFP_{714} dsRNA generated from pRNAi-GFP eliminates GFP_{714} expression and the infiltrated lamina show red auto-fluorescence. *DCL4* RNAi attenuated intracellular silencing and the level of PTGS decreased in *DCL4Ai*, *DCL4Bi*, and *DCL24i* plants. Some green fluorescence is still visible in the infiltrated lamina of these plants (G–I). Photographs were taken under long-wavelength UV light (top) or through a stereo-fluorescent microscope (bottom) at 4 dpa. Bar = 100 μm. The ratio in the bottom right corner of each panel indicates the number of plants out of the number of agro-infiltrated plants that developed local PTGS in two experiments. The green fluorescence intensity was measured using ImageJ software (Supplemental Fig. S4). J, Analysis of GFP_{714} mRNA in *DCL* RNAi lines. Northern detection was performed using GFP_{714}-specific probes (top). Equal loading of total RNAs extracted from leaf tissues at 4 dpa is indicated by the equal amount of 18S and 28S rRNAs shown on the gel (bottom). The position and size of GFP_{714} mRNA and 18S and 28S rRNA are indicated. K, Detection of local L-siRNAs. L-siRNAs were analyzed by small RNA northern blots (top). Equal loading of sRNAs extracted from leaf tissues at 4 dpa is indicated by the equal amount of 5S rRNA/tRNAs shown on gel (bottom). The position of 21, 22, and 24 nt siRNA as well as 5S rRNA/tRNAs are indicated.

reads was 5 to 8 times lower than that in *Nb*. In systemic leaves of *DCL3Ai* and *DCL3Bi* as well as those of *DCL4Ai* and *DCL4Bi*, only very low levels of 22 or 21 nt L-siRNAs were identified (Fig. 2, E–H, right), 45- to 68-fold lower than in *Nb*. The distribution across the GFP_{714} mRNA of both sense and antisense 21 to 24 nt L-siRNAs detected in local or systemic leaf tissues was almost identical among all samples (Fig. 3, left vs right panels A–I). However, we failed to detect any full-length or partial GFP_{714} RNA in systemic young leaves in any of the agro-infiltrated plants by RT-PCR using GFP_{714}-specific primers (Supplemental Fig. S7; Supplemental Table S5).

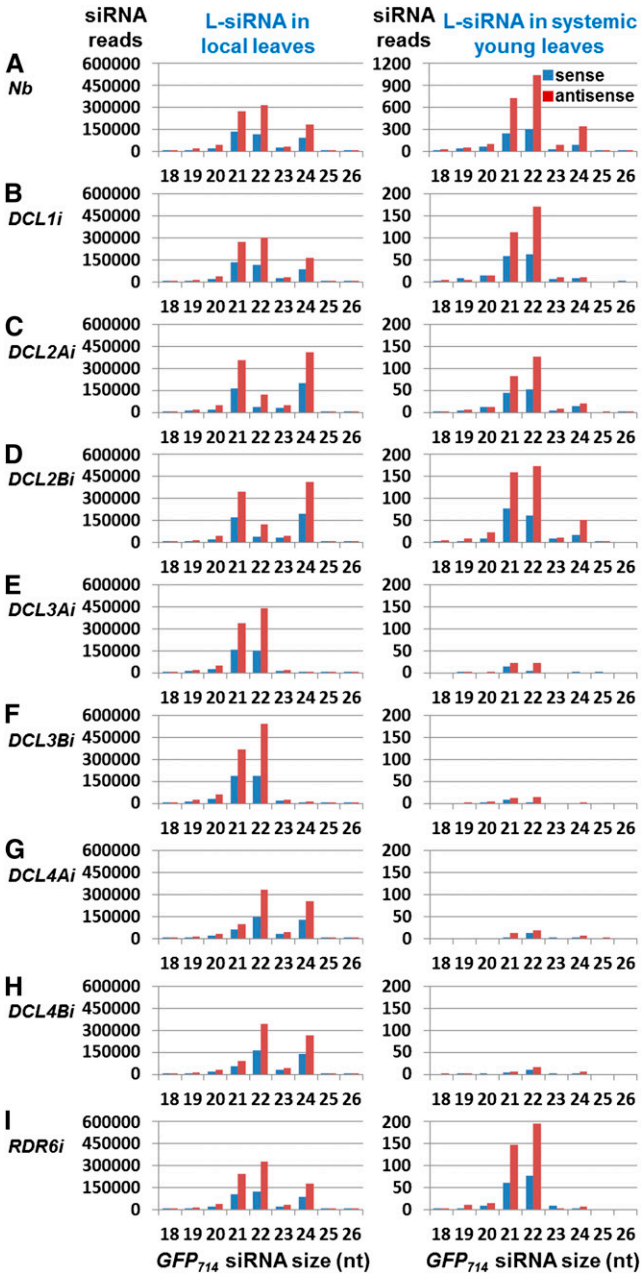

Figure 2. Detection of L-siRNAs in local and systemic leaves. A to I, GFP_{714} L-siRNAs generated from hairpin dsRNA-mediated local PTGS can be detected in distal systemic young leaves. Sense (blue) and antisense (red) 21, 22, and 24 nt L-siRNAs were present in local (left) and systemic (right) tissues of *N. benthamiana* (*Nb*, A) and RNAi lines *DCL1i* (B), *DCL2Ai* (C), *DCL2Bi* (D), *DCL3Ai* (E), *DCL3Bi* (F), *DCL4Ai* (G), *DCL4Bi* (H), and *RDR6i* (I). Outline of mobile siRNA assay is indicated in Supplemental Figure S3A.

DCL2 Facilitates, While *DCL4* and *DCL3* Attenuate, Systemic PTGS

To analyze the impact of *DCL* RNAi on systemic PTGS (Fig. 4), we infiltrated leaves of *Gfp* (resulting from a cross between *Nb* and *16cGFP*), *GfpDCL1i*, *GfpDCL2Ai*, *GfpDCL2Bi*, *GfpDCL3Ai*, *GfpDCL3Bi*, *GfpDCL4Ai*, or *GfpDCL4Bi* plants at the six-leaf stage with *Agrobacterium* harboring pRNAi-GFP_{714}. It is important to note that local PTGS is induced by the hairpin GFP_{714} that directly produces long dsRNA in the agro-infiltrated leaves. However, sense transgene GFP_{792} silencing in local and systemic young leaves requires the activity of multiple genes, including *RDR6*, to produce dsRNA from GFP_{792} ssRNA (Mlotshwa et al., 2008). Under long-wavelength UV light, we observed red fluorescence in halos around the infiltrated areas on *Gfp* and RNAi line leaves at 7 dpa (Fig. 4A; Supplemental Table S6), indicating local silencing.

DCL1 RNAi had no obvious effect on systemic silencing in *GfpDCL1i*; however, *DCL2* RNAi resulted in no PTGS in systemic young leaves of *GfpDCL2Ai* and *GfpDCL2Bi* (Fig. 4B; Supplemental Fig. S8; Supplemental Table S6). This contrasts with enhancement of systemic PTGS in *GfpDCL4Ai* and *GfpDCL4Bi* or *GfpDCL3Ai* and *GfpDCL3Bi* (Fig. 4B; Supplemental Fig. S8; Supplemental Table S6). Systemic silencing was further illustrated in single young leaves (Fig. 4, C–G). In contrast to the positive control (Fig. 4D), systemic PTGS was completely absent in the young leaves of *GfpDCL2Ai* and *GfpDCL2Bi*, as in *Gfp* (Fig. 4C). Only limited silencing was observed in one leaf located immediately above the infiltrated leaves at 18 dpa or later and such limited systemic PTGS was restricted to minor veins of *DCL2* RNAi plants (Fig. 4E). However, strong systemic silencing appeared in young leaves of *DCL3* and *DCL4* RNAi lines (Fig. 4, F and G). Similar results of *DCL* RNAi on local or systemic silencing were observed in *16cGFP*, *homGfpDCL2Ai*, *homGfpDCL3Bi*, and *homGfpDCL4Ai* plants as in *Gfp* and *GfpDCL* RNAi lines (Supplemental Table S6).

We then used northern hybridizations to detect systemic siRNA (dubbed Sy-siRNAs; Fig. 4H). Sy-siRNAs are siRNAs resulting from transitive silencing of the sense transgene GFP_{792} mRNA in nonagroinfiltrated leaves. Such systemic transitive silencing was triggered by mobile signals that were generated in agro-infiltrated local leaves. Sy-siRNAs also include two types of secondary siRNAs generated either from the GFP_{792} mRNA sequences that were directly targeted by the mobile signals or from the other parts of the GFP_{792} mRNA sequences that were not directly targeted by the mobile signals. No 21, 22, and 24 nt Sy-siRNAs were detected in the young leaves of *GfpDCL2Ai* and *GfpDCL2Bi* by northern blot (Fig. 4H). We were also unable to detect 24 nt Sy-siRNA in *GfpDCL3Ai* and *GfpDCL3Bi*, in which systemic silencing was apparently enhanced (Fig. 4, B, F, and H; Supplemental Fig. S8). However, 21, 22, and 24 nt Sy-siRNAs accumulated to a higher level in systemic leaves of *GfpDCL4Ai* and *GfpDCL4Bi* plants compared to *Gfp* (Fig. 4H). Considering the differential functions of *DCL4* and *DCL2* in primary and secondary siRNA biosynthesis (Chen et al., 2010; Cuperus et al., 2010), and the up-regulated *DCL2* expression in the *DCL4* or *DCL3* RNAi lines (Qin et al., 2017), we suspect that these Sy-siRNAs are

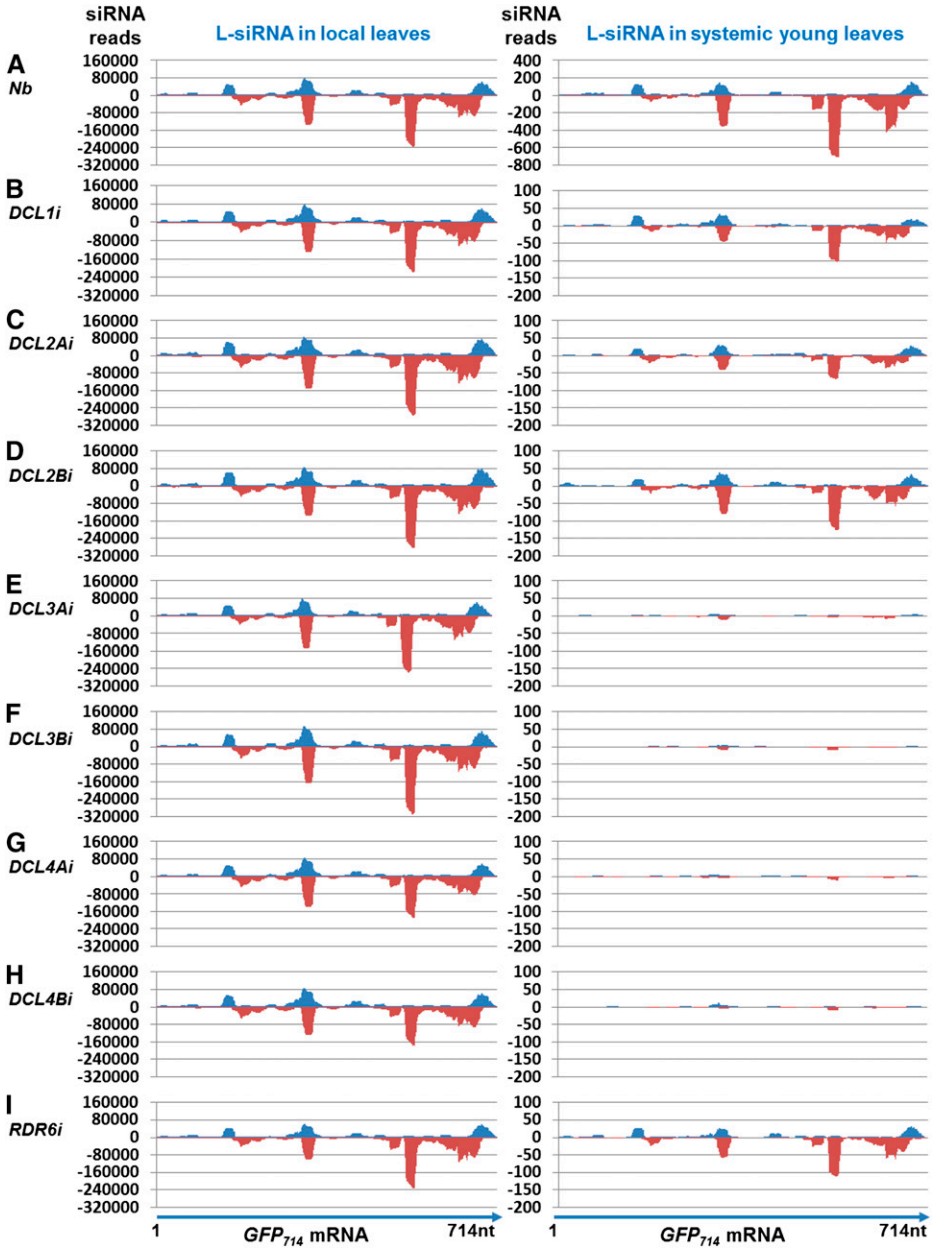

Figure 3. Distribution of 20 to 25nt L-siRNAs across the GFP_{714} mRNA. A to I, Distribution of 20 to 25nt GFP_{714} L-siRNAs for *N. benthamiana* (*Nb*; A); *DCL1i* (B); *DCL2Ai* and *DCL2Bi* (C and D); *DCL3Ai* and *DCL3Bi* (E and F); *DCL4Ai* and *DCL4Bi* (G and H); and *RDR6i* (I). Total GFP_{714} L-siRNA reads are from sRNA libraries of agro-infiltrated leaves (7 dpa; left) and systemic young leaves (14 dpa; right). Outline of mobile siRNA assay is indicated in Supplemental Figure S3A.

secondary siRNAs generated from the sense-transgene GFP_{792} mRNA. Taken together, our data demonstrate that *DCL2* facilitates, while *DCL4* and *DCL3* attenuate, systemic PTGS, at least for the transgene-induced PTGS in *N. benthamiana*.

Genetic Interplay between *DCL4* and *DCL2* to Influence Systemic PTGS

To investigate a potential genetic link between *DCL2* and *DCL4* in systemic PTGS (Fig. 4, I and L), we infiltrated leaves of the triple-cross *GfpDCL24Ai* and *GfpDCL24Bi* (Table I) with *Agrobacterium* harboring pRNAi-GFP_{714} at the six-leaf stage. Local RNA silencing was sufficiently induced, as evidenced by the appearance of red halos around the agro-infiltrated lamina (Fig. 4Ji). No long-distance spread of PTGS occurred to reach systemic leaves, which showed uniform green fluorescence under long-wavelength UV light (Fig. 4J, ii and iii; Supplemental Table S6), although some minor vein-restricted silencing was observed in one leaf immediately above the agro-infiltrated leaves (Fig. 4I). Similar systemic PTGS patterns were also found in an additional *DCL2-DCL4* double RNAi line *GfpDCL24Ci* (Table I; Supplemental Table S6). These findings show that *16cGFP* plants with simultaneous RNAi against *DCL2* and *DCL4* develop systemic PTGS in a manner similar to *GfpDCL2Ai* and *GfpDCL2Bi* lines, but in contrast to *GfpDCL4Ai* and *GfpDCL4Bi* lines.

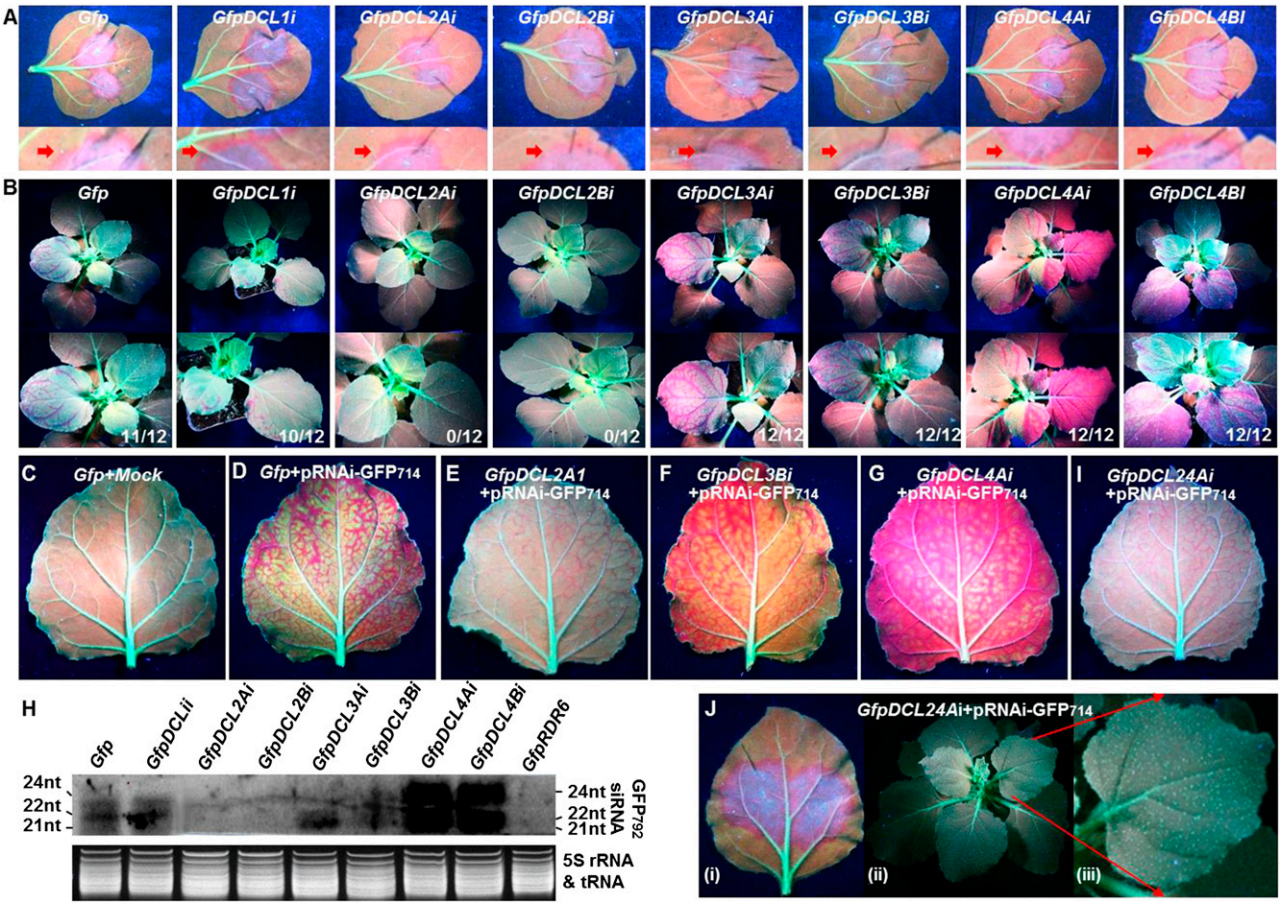

Figure 4. Antagonistic roles of *DCL2* against *DCL3* and *DCL4* in systemic PTGS. A and B, Impact of *DCL* RNAi on local and systemic PTGS. Local *GFP* silencing was induced by the hairpin GFP_{714} dsRNA in all plants by infiltration of leaves with agrobacterium harboring pRNAi-GFP_{714}, evident by the red halos around the infiltrated lamina. A close-up of the red halo (red arrow) below each image shows clearer silencing effects (A). Sense transgene GFP_{792}-mediated systemic PTGS was assessed on young leaves (B). At 14 dpa, all infiltrated plants of *GfpDCL4Ai* and *GfpDCL4Bi* lines developed very strong systemic GFP_{792} PTGS in young leaves. *GfpDCL3Ai* and *GfpDCL3Ai* plants also developed strong systemic PTGS in young leaves, although some relatively weak GFP_{792} silencing was observed in some *Gfp* and *GfpDCL1i* plants, and no systemic silencing appeared on any *GfpDCL2Ai* and *GfpDCL2Bi* plants. An enlarged snapshot (lower) of each photograph in its panel shows a clearer image of the silencing phenotypes (B). The ratio in the bottom right corner of each photo in B indicates the number of plants out of the number of agro-infiltrated plants that developed systemic PTGS in two separate experiments. Photographs were taken at 7 (A) and 14 dpa (B). C to G, Systemic transgene GFP_{792} silencing in young leaves. Transgene GFP_{792} expression was not silenced in the mock-infiltrated *Gfp* plant, and uniform green fluorescence occurred in the whole lamina of the noninfiltrated young leaf (C). Systemic GFP_{792} silencing in young leaf of *Gfp* plants infiltrated with agrobacterium harboring pRNAi-GFP_{714} was evident by the red fluorescence of chlorophyll across the leaf lamina of a newly grown young leaf (D). Only very weak GFP_{792} silencing was observed in the minor veins of a leaf immediately above the infiltrated leaves of *GfpDCL2Ai* (E), but extremely strong systemic GFP_{792} silencing appeared in *GfpDCL3Bi* (F) and *GfpDCL4Ai* (G). I, Weak minor vein-restricted systemic silencing in *GfpDCL24Ai*. Photographs were taken at 18 dpa. H, Northern-blot detection of Sy-siRNAs in the systemic young leaves at 14 dpa. Total sRNA extracted from systemic leaves of *GfpRDR6i* plants that were agro-infiltrated with pRNAi-GFP_{714} was included as a negative control. Top: siRNA blot, bottom: 5S rRNA/tRNA control showing equal loading of sRNA samples. The sizes and positions of siRNAs and 5S rRNA/tRNA are indicated. J, Local (i) and systemic (ii, iii) GFP_{792} silencing in *GfpDCL24Ai*. A section of Jii is enlarged to show a clearer young leaf image (Jiii). Photographs were taken at 7 dpa (Ji) or 14 dpa (Jii and iii). Influence of *DCL* RNAi on the development of local and systemic transgene GFP_{792} silencing is also summarized in Supplemental Table S6.

Comparison of Hairpin GFP_{714} and Transgene GFP_{792} Sequences

As indicated in Figure 5, sequences of transgene 792nt-GFP_{792} (Haseloff et al., 1997; Ruiz et al., 1998) in all transgenic *Gfp* and *GfpDCL* RNAi lines and hairpin 714nt-GFP_{714} (Ryabov et al., 2004) in the pRNAi-GFP_{714} vector share three identical and two less-similar regions, the latter named Region 1 and Region 2, respectively. GFP_{792} also possesses nucleotides 1 to 66 and 778 to 792 at both 5′-and 3′-ends that are completely

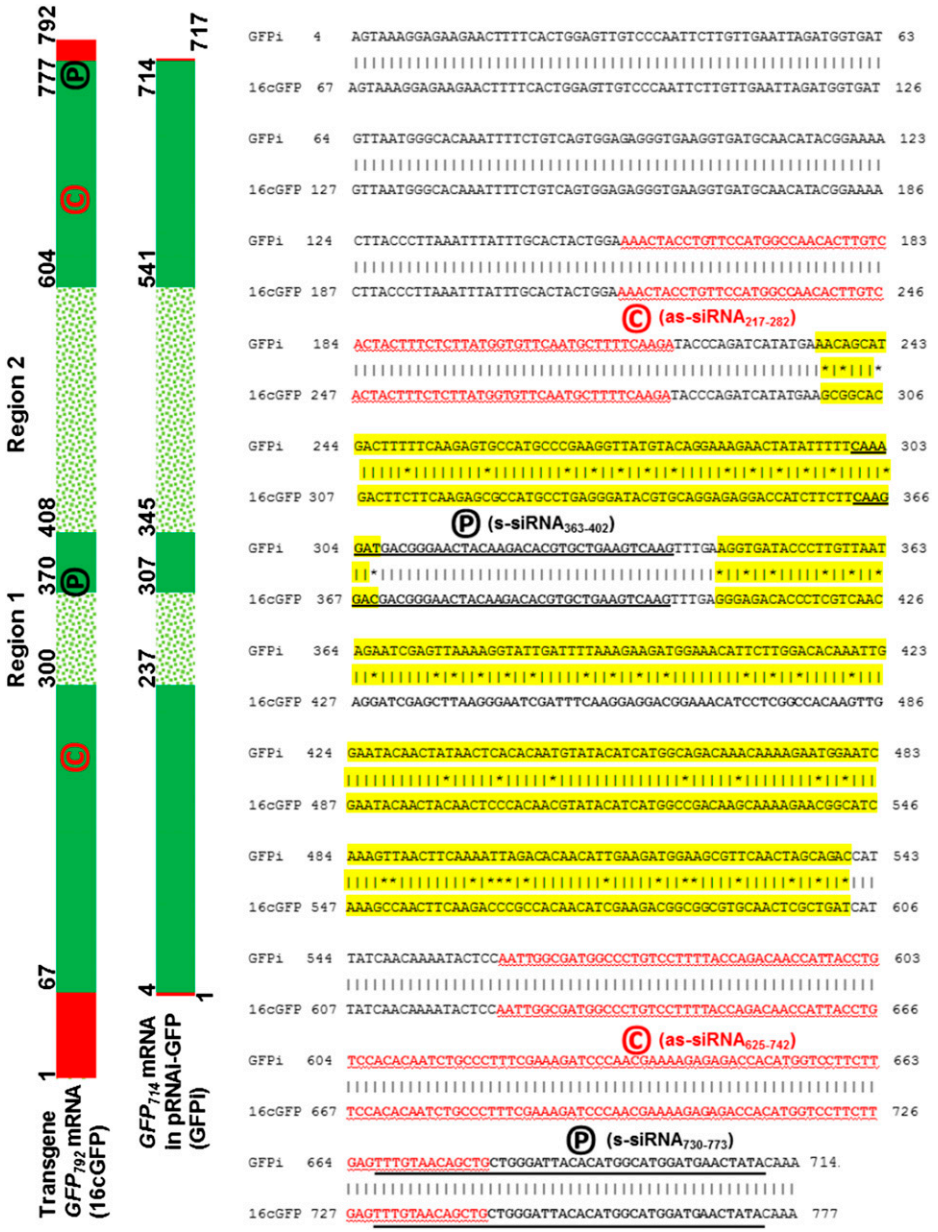

Figure 5. Comparisons of the transgene GFP_{792} and the hairpin GFP_{714} sequences. Completely distinct sequences between the GFP_{792} transgene (16cGFP) present in the *Gfp* and *GfpDCL* RNAi lines and the hairpin GFP_{714} (GFPi) in the pRNAi-GFP vector are outlined in red boxes, identical sequences are in green boxes, and similar sequences are in dotted boxes (highlighted yellow for the actual sequences). Sequence coordinates are indicated. The four clusters of the sense (s) and antisense (as) siRNAs corresponding to the positive (p) and complementary (c) stands (underlined) of the GFP_{714} and GFP_{792} mRNA are also indicated.

absent from the GFP_{714} sequence. Within Region 1 or Region 2, the maximum interval between any two consecutive mismatched bases is 14 nt. This information is essential and relevant to our subsequent siRNA profiling and bioinformatic analyses of siRNAs that may or may not be associated with transitive silencing. We only counted 20 to 25 nt siRNAs that were perfectly (100%) matched to target gene mRNAs. This means that the 20 to 25 nt siRNAs mapped to Region 1/Region 2 of the GFP_{792} mRNA will not be mapped to the equivalent Region 1/Region 2 of the GFP_{714} mRNA, or vice versa. Thus, these siRNAs are exclusive to either GFP_{792} or GFP_{714}, and most importantly, any Sy-siRNA unique to the transgene GFP_{792} Region 1/Region 2 mRNA should be generated by transitive silencing in systemic tissues.

Mapping L-siRNAs and Sy-siRNAs to Transgene GFP_{792} mRNAs and to Hairpin GFP_{714} dsRNA

To investigate whether L-siRNAs are associated with Sy-siRNA biosynthesis and systemic PTGS in distal recipient tissues, we performed systemic transgene GFP_{792} silencing assays (Supplemental Fig. S9A) and sequenced sRNA libraries generated from the infiltrated or systemic leaves of *Gfp*, *GfpDCL1i*, *GfpDCL2Ai*, *GfpDCL3Bi*, *GfpDCL4Ai*, and *GfpDCL24Ai* plants. Systemic transgene GFP_{792} silencing was triggered by mobile signals originating from local PTGS that was initiated by the hairpin GFP_{714} dsRNA (Fig. 4; Supplemental Fig. S9B). Similar to the sRNA results obtained from the non*GFP*-transformed RNAi lines, we

generated approximately 12 million sRNA reads for each library (Supplemental Table S7). Interrogation of these sRNA datasets further confirmed *DCL*-specific RNAi and their roles in siRNA biogenesis (Supplemental Figs. S9, B–P and S10). Moreover, RNAi of *DCL1* resulted in a clear reduction of miRNAs, although the total number of miRNAs was generally higher in systemic leaves than in local infiltrated leaves (Supplemental Fig. S11).

We mapped L- and Sy-siRNAs onto the transgene GFP_{792} mRNA. The distribution of antisense L- and Sy-siRNAs mapped to nucleotides 217-282 and 625-742 (Fig. 5, (c)-labeled) were essentially the same and sense L- and Sy-siRNAs mapped to nucleotides 363 to 402 and 730 to 773 of the transgene GFP_{792} mRNA (Fig. 5, (p)-labeled) in both local and systemic leaves of *Gfp* (Fig. 6, A and B), *GfpDCL1Ai* (Fig. 6, C and D), *GfpDCL2Ai* (Fig. 6, E–G), *GfpDCL3Bi* (Fig. 6, H and I), *GfpDCL4Ai* (Fig. 6, J and K), and *GfpDCL24Ai* (Fig. 6, L–N). The L-siRNAs in these four clusters (Fig. 6, A, C, E, H, J, and L; asterisked) corresponded to the occurrence of systemic GFP_{792} PTGS (Fig. 4; Supplemental Fig. S9B). We also found relatively high numbers of Sy-siRNA reads in young leaves where strong systemic GFP_{792} PTGS occurred in *Gfp*, *GfpDCL1i*, *GfpDCL3Bi*, and *GfpDCL4Ai* (Fig. 6, B, D, I and K). However, between the *Gfp* control and each of *GfpDCL* RNAi lines, we observed distinct profiles of L- and Sy-siRNAs across Region 1/Region 2 of the transgene GFP_{792} mRNA. Sy-siRNAs in young leaves specifically mapped to Region 1/Region 2 (Fig. 6, B, D, F, G, I, K, M, and N) were absent in the agro-infiltrated leaves where local silencing occurred efficiently in *Gfp*, *GfpDCL1i*, *GfpDCL2Ai*, *GfpDCL3Bi*, *GfpDCL4Ai*, and *GfpDCL24Ai* (Fig. 6, A, C, E, H, J, and L).

We also mapped the L- and Sy-siRNAs across the GFP_{714} mRNA, which was only expressed from pRNAi-GFP_{714} and formed hairpin dsRNA in the agro-infiltrated leaf lamina of *Gfp* (Fig. 7, A and B), *GfpDCL1i* (Fig. 7, C and D), *GfpDCL2Ai* (Fig. 7, E–G), *GfpDCL3Bi* (Fig. 7, H and I), *GfpDCL4Ai* (Fig. 7, J and K), and *GfpDCL24Ai* (Fig. 7, L–N). All four clusters of siRNAs mapped to the transgene GFP_{792} mRNA nucleotides 217 to 282, 363 to 402, 625 to 742, and 730 to 773, which also mapped to the equivalent identical sequences of the GFP_{714} RNA. However, L-siRNAs originating from the hairpin GFP_{714} dsRNAs were more abundant than the Sy-siRNAs derived from the transgene GFP_{792} mRNA. Moreover, we were able to map some L-siRNAs to Region 1 (nucleotide 237–306) and Region 2 (nucleotide 354–540) of the hairpin GFP_{714} RNA (Fig. 7, A, C, E, H, J, and L). These two regions differ from equivalent nucleotides 300 to 369 and 409 to 603 of the transgene GFP_{792} mRNA (Fig. 5). Intriguingly, only extremely low reads of such L-siRNAs were found in systemic leaves (Fig. 7, B, D, F, G, I, K, M, and N).

Taken together, these data (Figs. 5–7) suggest that (1) the hairpin GFP_{714} dsRNA is the main source for biogenesis of L-siRNA in local PTGS; (2) GFP_{714}-specific L-siRNAs mapped to Regions 1/2 are present in systemic leaf tissues; (3) L-siRNAs are associated with the Sy-siRNA biogenesis and the induction of systemic GFP_{792} silencing; and (4) Sy-siRNAs unique to the two specific regions, that is Regions 1/2 of the transgene GFP_{792} mRNA, are generated by transitive silencing in systemic young leaves.

Influence of *DCLs* on Biogenesis of 21, 22, and 24 nt L-siRNAs for Systemic Transgene GFP_{792} Silencing

To further examine the association of L-siRNAs with systemic GFP_{792} PTGS in *Gfp* (Fig. 8, A and B), *GfpDCL1i* (Fig. 8, C and D), *GfpDCL2Ai* (Fig. 8, E–G), *GfpDCL3Bi* (Fig. 8, H and I), *GfpDCL4Ai* (Fig. 8, J and K), and *GfpDCL24Ai* (Fig. 8, L–N), we analyzed the size distribution of sense and antisense L- and Sy-siRNAs (Fig. 8). In local silencing induced by the hairpin GFP_{714} dsRNA, there were generally more antisense than sense L-siRNAs (Fig. 8, A, C, E, H, J, and L). However, in systemic GFP_{792} PTGS, sense- and antisense Sy-siRNAs were approximately equal (Fig. 8, B, D, F, G, I, K, M, and N). Furthermore, the distribution of 21, 22, and 24 nt L-siRNAs differed from that of Sy-siRNAs in infiltrated and systemic leaves for *Gfp* (Fig. 8, A and B), *GfpDCL1i* (Fig. 8, C and D), *GfpDCL2Ai* (Fig. 8, E–G), *GfpDCL3Bi* (Fig. 8, H and I), *GfpDCL4Ai* (Fig. 8, J and K), and *GfpDCL24Ai* (Fig. 8, L–N).

In *Gfp* and *GfpDCL1Ai*, the siRNA profile was almost identical, but shifted from 22, 21, and 24 nt L-siRNAs (approximately 2.5:2:1 ratio for sense L-siRNA and about 1.4:1.2:1 for antisense L-siRNA) for local silencing to predominantly 21 nt along with some 22 nt (approximately 6 fold less than 21 nt) and low level of 24 nt (around 300 times less than 21 nt) Sy-siRNAs for systemic PTGS (Fig. 8, A–D). However, RNAi of *DCL2*, *DCL3*, and *DCL4* had different impacts on the accumulation of 21, 22, and 24 nt L- and Sy-siRNAs. In local silencing, high levels of 24 and/or 21nt L-siRNAs were generated in *GfpDCL2Ai* and *GfpDCL24Ai* (Fig. 8, E and L). Only a very low level of Sy-siRNAs (10^3–10^5 fold less than L-siRNAs) was found in young leaves, which showed no systemic silencing (Fig. 8, G and N), although 100 to 200 or less of 21, 22, and 24 nt Sy-siRNAs were detected in leaves with minor vein-restricted systemic PTGS (Fig. 8, F and M). The decrease in the 22 nt L-siRNAs was closely correlated with the decrease in the levels of Sy-siRNAs, as well as with the abolition and/or reduction of systemic GFP_{792} silencing in young leaves of *GfpDCL2Ai* and *GfpDCL24Ai* (Fig. 4; Supplemental Figs. S8 and S9B).

By contrast, the enhanced systemic transgene GFP_{792} PTGS and the increased Sy-siRNA reads in young leaves were positively linked with the elevated levels of 22 nt L-siRNAs in local tissues of *GfpDCL3Ai* (Fig. 8H) and *GfpDCL4Ai* (Fig. 8J). However, we observed a reduction in the level of 24 nt L-siRNAs (nearly none) in *GfpDCL3Bi* (Fig. 8H) as well as a decrease in 21 nt L-siRNAs (3- to 4-fold less than 22 nt L-siRNAs) in

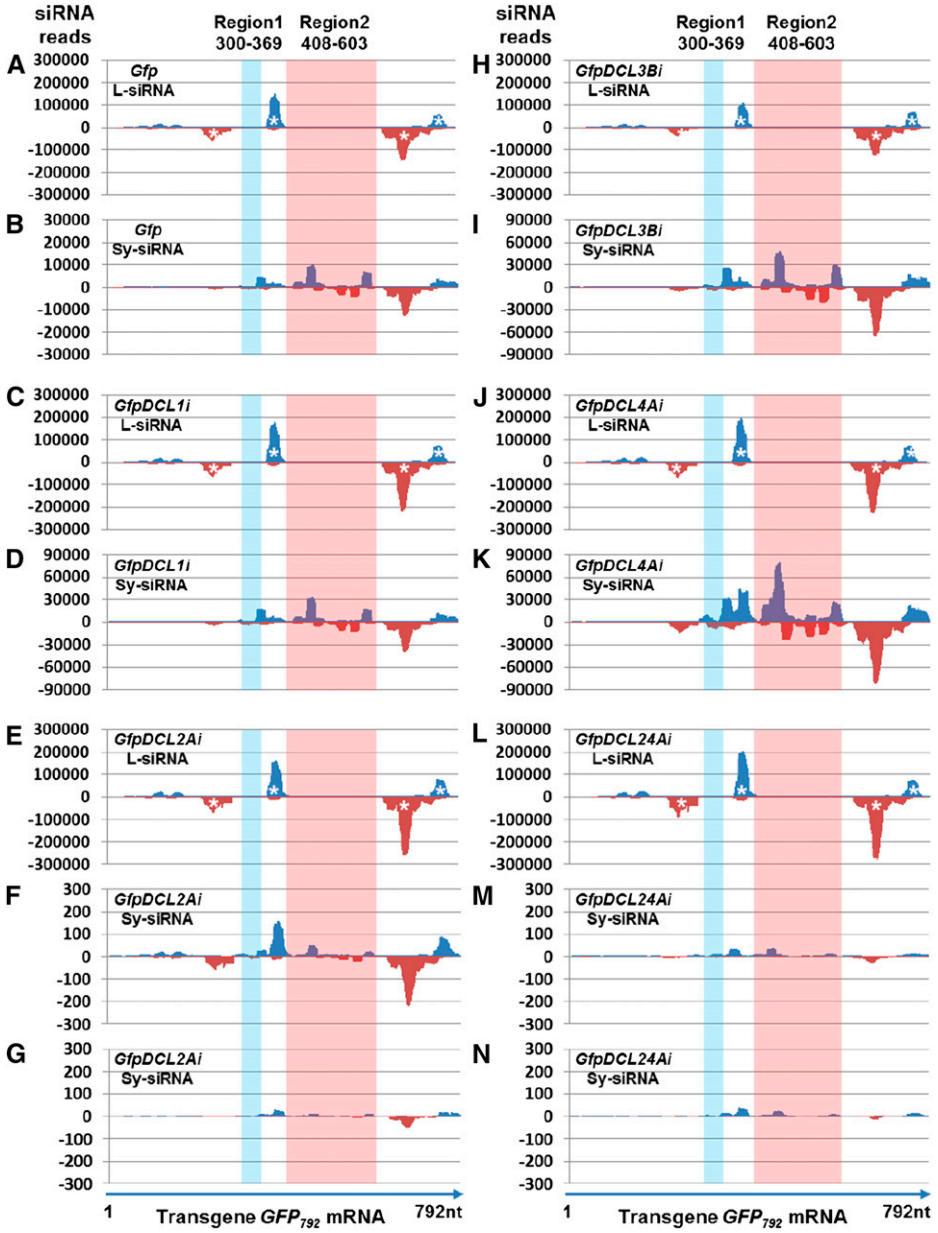

Figure 6. Distribution of L- and Sy-siRNA across the transgene GFP_{792} mRNA. A and B, *Gfp*. C and D, *GfpDCL1i*. E to G, *GfpDCL2Ai*. H and I, *GfpDCL3Bi*. J and K, *GfpDCL4Ai*. L to N, *GfpDCL24Ai*. Total L- and Sy-siRNAs are from local agro-infiltrated leaves (A, C, E, H, J, and L) and systemic young leaves (B, D, F, G, I, K, M, and N). Sense- (blue) and antisense (red) siRNAs were mapped to the transgene GFP_{792} mRNA sequence. The profiles of L-siRNAs generated largely from the hairpin GFP_{714} dsRNA differ from that of Sy-siRNAs that were derived from the GFP_{792} mRNA, particularly in the two less similar Region 1/Region 2 (Fig. 5). These differences indicate that elevated levels of L-siRNAs (*) together with their long RNA precursor RNAs, despite the latter being unlikely (Supplemental Fig. S7), moved from local to systemic leaves and contributed to silencing signal. Such mobile signals might act as the primary trigger for production of Sy-siRNAs and for systemic transgene GFP_{792} silencing in distal young leaves. Sense and antisense Sy-siRNAs associated with Region 2 and Region 1 (highlighted) in systemic recipient cells are likely secondary and resulted from transitive silencing. Experimental design for systemic silencing assays is indicated in Supplemental Figure S9A. Systemic transgene GFP_{792} PTGS are shown in Figure 4, Supplemental Figure S8, and Supplemental Figure S9B. Compared to *Gfp* (B) and *GfpDCL1i* (D), strong systemic PTGS occurred in *GfpDCL3Bi* (I) and *GfpDCL4i* (K); no systemic PTGS was observed in young leaves of *GfpDCL2Ai* (F) and *GfpDCL24Ai* (M), and only very weak vein-restricted silencing in the leaf located immediately about the agro-infiltrated leaves of *GfpDCL2Ai* (G) and *GfpDCL24Ai* (N).

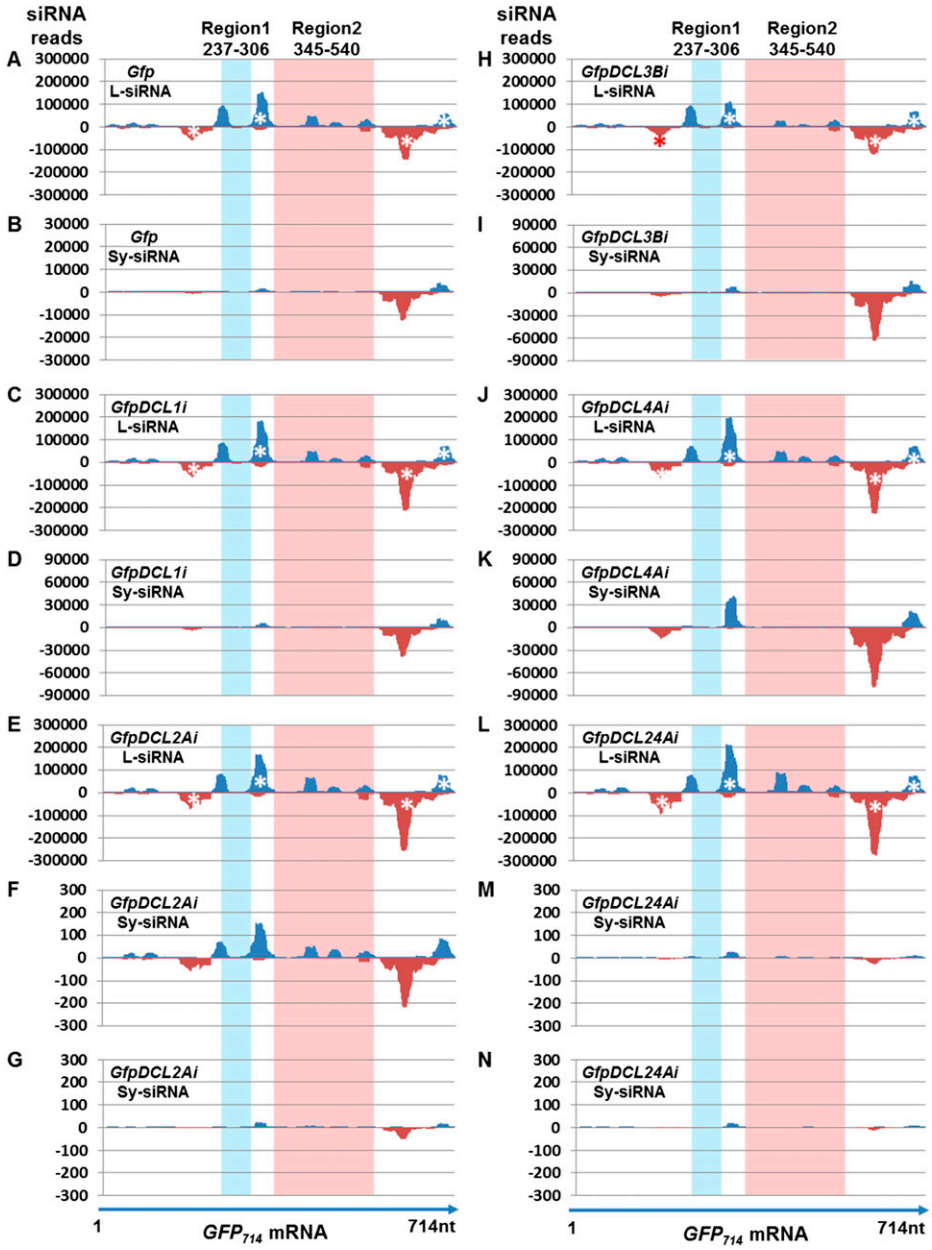

Figure 7. Distribution of L- and Sy-siRNAs across the hairpin GFP_{714} RNA. A and B, *Gfp*. C and D, *GfpDCL1i*. E to G, *GfpDCL2Ai*. H and I, *GfpDCL3Bi*. J and K, *GfpDCL4Ai*. L to N, *GfpDCL24Ai*. Total L- or Sy-siRNAs are from local agro-infiltrated leaves (A, C, E, H, J, and L) or systemic young leaves (B, D, F, G, I, K, M, and N). Sense- (blue) and antisense (red) siRNAs were mapped to the hairpin GFP_{714} RNA. The L-siRNA profiles differ from Sy-siRNAs in the two less similar Region 1/Region 2 (Fig. 5). Experimental design for systemic silencing assays is indicated in Supplemental Figure S9A. Systemic transgene GFP_{792} PTGS are shown in Figure 4, Supplemental Figure S8, and Supplemental Figure S9B.

GfpDCL4Ai (Fig. 8J), consistent with sRNA northern detection (Fig. 4H). Further siRNA size profiling confirmed that the levels of 22 nt L-siRNA were linked with efficient systemic transgene GFP_{792} PTGS, whereas variations in 21 and 24 nt L-siRNAs did not affect Sy-siRNA production and the occurrence of systemic GFP_{792} silencing (Supplemental Fig. S12).

Requirement of *DCL2* to Respond to Mobile Systemic PTGS

To further investigate the genetic mechanism involved in the control of systemic PTGS, we used *16cGFP*, *homGfpDCL4Ai*, and *homGfpDCL2Ai* (Table I) as either rootstocks or scions in reciprocal grafting experiments (Fig. 9). When grafted onto the sense transgene GFP_{792}-silenced *homGfpDCL4Ai* stocks, *homGfpDCL2Ai* scions developed no PTGS and showed strong GFP green fluorescence (Fig. 9, A and B). However, in the reciprocal grafting, strong sense transgene-mediated PTGS occurred in *homGfpDCL4Ai* scions 3 weeks after grafting (wag), even if *homGfpDCL2Ai* stocks had very limited transgene GFP_{792} silencing (Fig. 9C, inlet). In controls, efficient PTGS took place at 3 wag in *homGfpDCL4Ai* scions that were grafted onto GFP_{792}-silenced *homGfpDCL4Ai* stocks (Fig. 9D). In a different experimental setting, *homGfpDCL2Ai* scions grafted

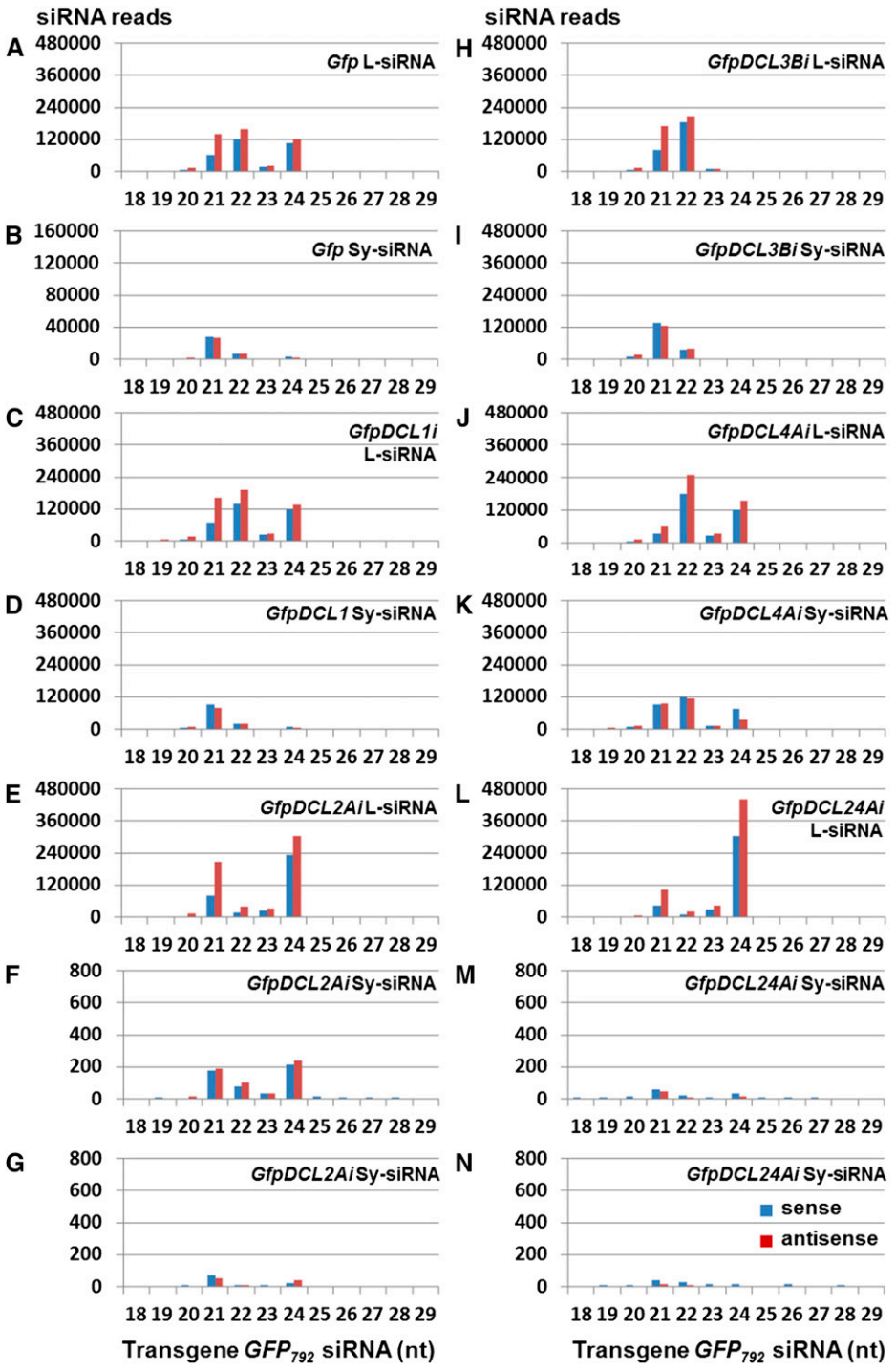

Figure 8. Size profiles for L- and Sy-siRNAs. A to N, Fourteen sRNA libraries were generated from sRNA samples extracted from agroinfiltrated leaves at 7 dpa (A, C, E, H, J, and L) and systemic young leaves at 14 dpa (B, D, F, G, I, K, M, and N) of *Gfp* (A and B), *GfpDCL1i* (C and D), *GfpDCL2Ai* (E–G), *GfpDCL3Bi* (H and I), *GfpDCL4Ai* (J and K), and *GfpDCL24Ai* (L–N). Plants were infiltrated with agrobacterium harboring pRNAi-GFP$_{714}$. Blue and red bars represent L- and Sy-siRNAs aligned to the sense and antisense strand of *GFP*$_{792}$ mRNA, respectively. The abundance of the 22-nt L-siRNA is closely correlated with the induction and reduction of systemic transgene *GFP*$_{792}$ silencing in systemic young leaves. Experimental design for systemic silencing assays is indicated in Supplemental Figure S9A. Systemic transgene *GFP*$_{792}$ PTGS are shown in Figure 4, Supplemental Figure S8, and Supplemental Figure S9B.

onto presilenced *16cGFP* stocks remained unsilenced throughout the experiments, while *homGfpDCL4Ai* scions developed systemic PTGS at 3 wag (Fig. 9, E and F). These results demonstrate that (1) *DCL4* is unlikely required to produce and respond to mobile silencing signals for systemic PTGS, and (2) *DCL2* is required in the scion to respond to the signal, but not in the rootstock to produce/send the signal.

DISCUSSION

Genetic insights into mobile RNA silencing and involvement of mobile signal(s) in systemic silencing remain two of the least understood, but yet most debated and divisive topics in the field of plant RNA silencing. Using a suite of *DCL* RNAi lines together with a GFP reporter, grafting, sRNA hybridization, and NGS

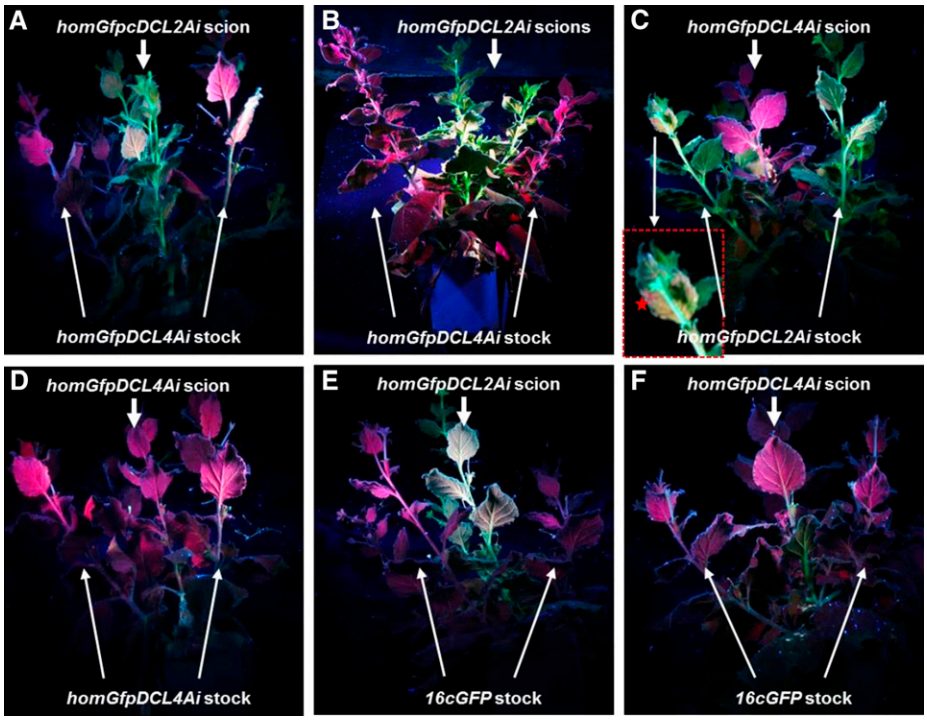

Figure 9. Systemic silencing in grafted *homGfpDCL2Ai* and *homGfpDCL4Ai* plants. A and B, *16cGFP*, *homGfpDCL2Ai*, and *homGfpDCL4Ai* plants were used as silenced stocks to produce or as scions to receive systemic silencing signals in three experiments. No systemic transgene GFP_{792} silencing was observed in *homGfpDCL2Ai* scions grafted onto GFP_{792}-silenced *homGfpDCL4Ai* stocks 3 wag (A) and 6-wag (B). C, Systemic GFP_{792} silencing at 3 wag in a *homGfpDCL4Ai* scion grafted onto a *homGfpDCL2Ai* stock. An enlarged section (boxed) of the stock plant showed very limited GFP_{792} silencing with red fluorescence marked with an asterisk in the inset leaf. D, Systemic GFP_{792} silencing in a *homGfpDCL4Ai* scion grafted onto a GFP_{792}-silenced *homGfpDCL4Ai* stock at 3 wag as a control. E, A *homGfpDCL2Ai* scion grafted onto GFP_{792}-silenced *16c* stocks remained unsilenced at 3 wag and afterward. F, Systemic transgene GFP_{792} silencing in a *homGfpDCL4Ai* scion grafted onto a GFP_{792}-silenced *16cGFP* stock at 3 wag. All plants are photographed under long-wavelength UV illumination. Red fluorescence shows transgene GFP_{792} silencing while green fluorescence indicates no silencing. Scions and stocks are indicated by arrows in each panel.

approaches, we have found that gene-specific suppression of *DCL2* expression reduces systemic PTGS. *DCLs* play central roles in the biogenesis of 21, 22, and 24 nt antisense and sense L-siRNAs in incipient cells. *DCL2* is required to respond to mobile signals in recipient cells, but to produce such signals in incipient cells. *DCL4* or *DCL3* inhibit non-cell autonomous PTGS in systemic tissues. We also extensively profiled L- and Sy-siRNAs associated with both local hairpin dsRNA-mediated silencing and systemic transitive sense-transgene PTGS and examined how L-siRNAs generated by DCLs affect long-distance spread of PTGS. We propose that *DCL2* is the key player along with *DCL4* and *DCL3*, as well as mobile siRNAs in systemic PTGS (Fig. 10). Thus, we report several novel findings that shed light on how systemic PTGS is genetically and molecularly regulated in *N. benthamiana*.

1. We have generated transgenic *DCL* RNAi lines for dissecting intra/intercellular and systemic PTGS (Table I). *DCL1*, *DCL2*, *DCL3*, and *DCL4* are responsible for the biogenesis of miRNAs and 22, 24, and 21 nt siRNAs, respectively, in *N. benthamiana*. *DCL4* and the DCL4-processed 21 nt siRNAs are essential for local hairpin dsRNA-mediated PTGS, while *DCL2* or *DCL3* and their cognate 22 or 24 nt L-siRNAs are not critical for such intracellular silencing (Fig. 1).
2. Local PTGS induced by the hairpin GFP_{714} dsRNA can lead to efficient biogenesis of mobile L-siRNAs in incipient cells and local leaf tissues (Figs. 1–3). Our experimental system (Supplemental Fig. S3A) avoids the amplification and cascading production of siRNAs in remote recipient cells and enables unambiguous detection of different sized L-siRNAs in systemic leaves. However, neither long (full-length or partial) GFP_{714} RNA (Supplemental Fig. S7) nor agrobacterium-originated siRNA (Supplemental Table S2) was detectable in young leaves, although these results do not rule out the possibility that long RNAs are present and serve as the mobile signal. Moreover, the total number of GFP_{714} L-siRNA (and

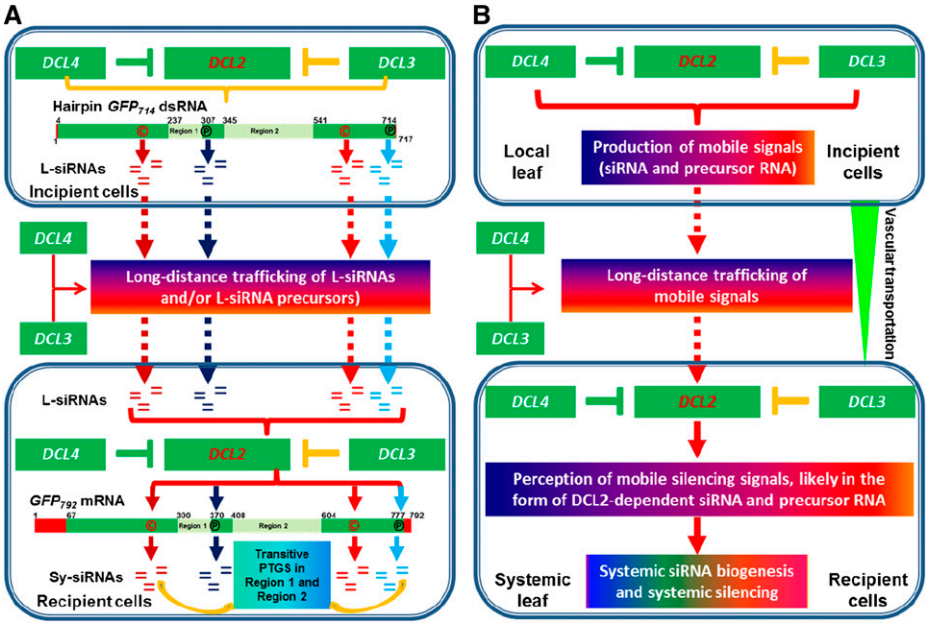

Figure 10. Systemic PTGS in *N. benthamiana*. A, A regulatory complex among *DCL2*, *DCL3*, and *DCL4* contributes to biogenesis of mobile silencing signals for systemic PTGS. Regulation of *DCL2* expression by *DCL4* or *DCL3* is demonstrated in our recent work (Qin et al., 2017). *DCL1* is not included, because it seems to have no obvious effect on systemic PTGS. In this model, mobile 21, 22, and 24 nt L-siRNAs are generated from the hairpin GFP_{714} dsRNA by DCL2, DCL3, or DCL4 in the incipient cells of local leaf tissues. However, only the levels of the DCL2-processed 22 nt L-siRNAs, particularly those L-siRNAs matching to the four identical regions indicated by (p) (positive strand) or (c) (complementary strand) of the hairpin GFP_{714} and the transgene GFP_{792} mRNA (Fig. 5), are somewhat correlated with the DCL2-dependent induction of systemic transgene GFP_{792} PTGS and Sy-siRNA biogenesis in the recipient cells of systemic leaf tissues. Sy-siRNAs unique to Region 1/Region 2 of the transgene GFP_{792} mRNA are generated by transitive PTGS in recipient cells. Different color "=" signs represent siRNAs matching to each of the four identical sequences between GFP_{714} and GFP_{792} (Fig. 5). B, *DCL2*-dependent *DCL* genetic network in systemic silencing. Reduction of *DCL2* reduces systemic PTGS, suggesting that *DCL2* acts an important activator of the long-distance spread of PTGS. *DCL2* is also required to perceive incoming signals, likely in the form of sense and antisense siRNAs and their long RNA precursor (although the latter is unlikely to contribute to systemic silencing), for induction of systemic siRNA biogenesis and execution of systemic PTGS in distal recipient cells. *DCL4* or *DCL3* may contribute to systemic silencing through their positive influences on long-distance movement of siRNAs; however, both are negative regulators (T sign) that down-regulate *DCL2* expression (Qin et al., 2017). Thus, *DCL2* is a key player in the systemic silencing network. Suppression of either *DCL4* or *DCL3* alleviates the negative control of *DCL2* expression and the elevated *DCL2* could then respond more effectively to mobile signals for more efficient systemic PTGS in *N. benthamiana*.

total sRNA) reads in local leaf tissues and their distributions across the GFP_{714} RNA are almost identical among *Nb*, *RDR6i*, and all *DCL* RNAi lines (Figs. 2 and 3). The L-siRNAs detected in systemic leaves are mainly 22 and 21 nt, but some are 24 nt (Fig. 2). These mobile L-siRNAs were not particularly abundant in systemic young leaf tissues, but consistent with the levels of mobile siRNAs reported in Arabidopsis (Molnar et al., 2010). These data indicate that all sized sense and antisense L-siRNAs are capable of trafficking over long distances (Fig. 10A). Compared to *Nb*, the reduced levels of L-siRNAs in distal tissues of all RNAi lines suggest that *RDR6* and *DCLs*, particularly *DCL3* and *DCL4*, contribute to the systemic spread of L-siRNAs (Fig. 2). Indeed, genetic analyses have demonstrated that *RDR6* is required for perception of long-distance silencing signals (Schwach et al., 2005; Melnyk et al., 2011b) and *DCL2* responds to mobile silencing for efficient systemic PTGS in plants (Fig. 4; Taochy et al., 2017). However, even if locally produced siRNAs are mobile, this does not prove that siRNAs are the signal.

3. Genetic analysis indicates that *DCL1* is unlikely to be involved in local hairpin dsRNA-mediated PTGS, although a slightly elevated level of target mRNA was detected in *DCL1i* plants (Fig. 1) and sense-transgene induced systemic PTGS (Figs. 4). This conclusion is supported by the identical profiles of L-siRNAs or Sy-siRNAs in both *Gfp* and *GfpDCL1i* plants (Figs. 6–8). Further, the altered size profiles between L- and Sy-siRNAs in *Gfp* and *GfpDCL1i* (Fig. 8) implies that the local and systemic PTGS are likely two linked processes with distinct molecular and genetic requirements. Indeed, local PTGS is induced by a hairpin GFP_{714} RNA that directly produces long dsRNA, which differs from the

sense transgene GFP_{792}-mediated PTGS in systemic leaf tissues. In the latter case, dsRNA is not produced directly, but its production from ssRNA requires the activity of several genes, including *RDR6* and *DCL2* (Mlotshwa et al., 2008).

4. *DCL2* RNAi reduces systemic PTGS and blocks the exit of the mobile silencing signal from vascular tissues to the surrounding mesophyll cells, indicating that *DCL2* is required for long-distance spread of PTGS (Fig. 4), consistent with *DCL2* promoting, while *DCL4* inhibits, cell-to-cell spread of VIGS (Qin et al., 2017). Moreover, *DCL2* is required to respond to mobile signals for systemic PTGS (Fig. 9), supported by a recent report of a critical role of DCL2 in systemic PTGS in Arabidopsis (Taochy et al., 2017). *DCL2* is thus involved in promoting the long-distance (leaf-to-leaf) and short-distance movement (vascular cells to neighboring cells) of PTGS in addition to its role in generating the 22 nt siRNAs. On the other hand, our grafting experiments showed that *DCL2* is not required in the rootstock for producing/sending the signal (Fig. 9). However, in contrast to complete loss-of-function mutants, RNAi lines are partial loss-of-function. It thus remains possible that in the *DCL2i* rootstock, residual *DCL2* could still produce some transportable molecules, and such signals could then be perceived by *DCL2* in recipient cells where *DCL4* is knocked-down by RNAi to trigger systemic transitive PTGS (Fig. 9). Taochy et al. (2017) have elegantly shown that Arabidopsis *DCL2* is required in both the source rootstock and recipient shoot tissue for RDR6-dependent systemic PTGS, although this latest discovery is in contrast to their previous finding (Brosnan et al., 2007).
5. Contrary to *DCL2*, *DCL4* and *DCL3* inhibit sense transgene-mediated systemic PTGS, as RNAi of *DCL4* or *DCL3* enhances systemic PTGS in distant young leaves (Fig. 4). Our data also reveal that *DCL4* has an epistatic effect on *DCL2*, thereby influencing systemic PTGS in *N. benthamiana* (Fig. 4, I and J). Only *DCL2* is required to respond to mobile signals for systemic PTGS in the reciprocal *DCL2i-DCL4i* grafting experiments (Fig. 9), and RNAi of *DCL4* or *DCL3* has been found to up-regulate *DCL2* expression (Qin et al., 2017). Taken together, our findings suggest that a *DCL2*-dependent *DCL* genetic network regulates non-cell autonomous systemic silencing (Fig. 10B). A hierarchical interaction between *DCL4* and *DCL2* to affect cell autonomous PTGS was also reported in Arabidopsis (Bouché et al., 2006; Henderson et al., 2006; Xie et al., 2005).
6. Our work implicates or excludes the involvement of certain types of RNAs in mobile systemic PTGS (Fig. 10A). First, combined with earlier elegant work showing that *DCL2* is required for transitive silencing (Mlotshwa et al., 2008; Parent et al., 2015), our results suggest that the plant's response to the signal requires a set of genes that are unique to transitive silencing (i.e. genes that play a role in the production of dsRNA). Thus, these results suggest that the signal for systemic silencing in plants is not itself dsRNA, in contrast to dsRNA being required for the systemic spread of RNAi in animals (Jose et al., 2011).

Second, detection of L-siRNAs in systemic tissues implies that mobile L-siRNAs might contribute to systemic PTGS. This notion is supported by the L- and Sy-siRNA profiles associated with the hairpin GFP_{714} dsRNA-mediated local silencing and systemic transgene GFP_{792} silencing. The identical distributions of the four clusters of L- and Sy-siRNAs across nucleotides 625 to 742 and 217 to 282, 730 to 773 and 363 to 402 of the transgene GFP_{792} mRNA and the equivalent sequences of the hairpin GFP_{714} dsRNA (Fig. 5, labeled (c) or (p)) suggest that L-siRNAs originated from these parts of the hairpin GFP_{714} dsRNA might represent a component of mobile signals for the biosynthesis of Sy-siRNA and for systemic induction of GFP_{792} silencing in distal recipient cells (Figs. 6 and 7, asterisk). Consistent with this, the abundance of the four clusters of Sy-siRNAs associated with systemic GFP_{792} PTGS are much less than the corresponding L-siRNAs associated with local silencing induced by the hairpin GFP_{714} dsRNA in control and all RNAi lines (Figs. 6 and 7, asterisk). Furthermore, L-siRNAs specific to Regions 1/2 of the hairpin GFP_{714} dsRNA were found in systemic leaf tissues (Fig. 7). By contrast, Sy-siRNAs unique to Regions 1/2 of the transgene GFP_{792} mRNA (these two regions have different sequences between GFP_{714} and GFP_{792}; Fig. 5) were not found in local leaves where primary silencing efficiently occurred (Fig. 6). These results suggest that Sy-siRNAs distinct to Regions 1/2 of the GFP_{792} mRNA must have been generated from transitive sense-transgene silencing in systemic leaf cells and tissues. Such transitive PTGS was likely induced by secondary siRNAs that were produced from primary silencing of the GFP_{792} mRNA sequences, directly targeted by the four clusters of mobile L-siRNAs that were generated from the identical GFP_{714} sequences in local PTGS (Figs. 6–8; Fig. 10A). However, these results do not exclude the possible involvement of other types of RNAs in systemic RNA silencing in plants.

Third, the 21 or 24 nt L-siRNAs processed by DCL4 or DCL3 and their precursor RNAs are unlikely to be a major component of the mobile signal for systemic PTGS (Fig. 8), in line with our genetic and functional analysis of *DCLs* in systemic silencing (Fig. 4). That suppression of *DCL4* or *DCL3* enhanced systemic silencing and the levels of 21 or 24 nt L-siRNAs were not correlated with the biogenesis of GFP_{792} Sy-siRNAs (Fig. 8) and the intensity of systemic PTGS in all *GfpDCL*

RNAi lines (Fig. 4) provides evidence to support such a conclusion. This is also consistent with the fact that DCL4 and DCL3 proteins are not required for the production of the sRNA signals in Arabidopsis (Brosnan et al., 2007; Taochy et al., 2017).

Fourth, the levels of DCL2-processed 22 nt L-siRNAs were weakly correlated with the induction of systemic PTGS. Mapping L- and Sy-siRNAs onto the transgene GFP_{792} mRNA and hairpin GFP_{714} dsRNA identified sense and antisense 22 nt L-siRNAs that might be required for systemic GFP_{792} PTGS in distal recipient cells. It is evident that the varied levels of the 22 nt L- and Sy-siRNAs mapped to the transgene GFP_{792} antisense sequences 625 to 742 and 217 to 282, and sense strand 730 to 773 and 363 to 402 (Supplemental Fig. S12) were linked to the induction of systemic GFP_{792} silencing in each RNAi lines (Fig. 4). This is also consistent with the high levels of 21, 22, and 24 nt Sy-siRNAs in *GfpDCL4Ai*, likely resulting from DCL2 and DCL2-processed 22 nt siRNAs that may trigger efficient biosynthesis of secondary Sy-siRNAs in the systemic leaf tissues (Chen et al., 2010; Cuperus et al., 2010; Mlotshwa et al., 2008). However, these findings per se are not direct evidence that DCL2-processed 22 nt L-siRNAs and/or their precursors are the *bona fide* signals for induction of Sy-siRNA biogenesis and systemic transitive PTGS.

Nonetheless, the molecular nature of systemic PTGS signals needs further characterization. DCL4-processed 21 nt siRNA or DCL3-processed 24 nt siRNA and their precursors may not be involved in long-distance PTGS signaling, even though 21 and 24 nt siRNAs act primarily as intra- or intercellular triggers for RNA-directed degradation of target mRNA or RNA-directed DNA methylation (Lewsey et al., 2016; Melnyk et al., 2011a, 2011b; Sarkies and Miska, 2014). In Arabidopsis, the DCL3-processed 24 nt siRNAs are thought to be the main signals for systemic TGS (Lewsey et al., 2016; Melnyk et al., 2011a; Molnar et al., 2010). However, we have not examined the roles of DCLs and mobile siRNAs in systemic TGS in *N. benthamiana*. Furthermore, whether the DCL2-processed/dependent 22 nt siRNAs and/or their precursors could serve as signals for systemic PTGS requires further investigation, even though 22 nt sRNAs can effectively trigger biogenesis of secondary siRNAs of various sizes in plants (Chen et al., 2010; Cuperus et al., 2010; Mlotshwa et al., 2008) and DCL2 and DCL2-processed 22 nt siRNAs are involved in the cell-to-cell spread of VIGS in *N. benthamiana* (Qin et al., 2017).

Our findings also differ from early works showing that long-distance movement of transitive silencing occurs in the absence of sRNAs in the rootstock (Mallory et al., 2001), and that no specific sRNAs are associated with systemic silencing in Arabidopsis (Brosnan et al., 2007; Taochy et al., 2017). Considering the transitivity and sequence-specificity of RNA silencing along with the fact that various types of RNA molecules can trigger cell-autonomous silencing, we concede that various forms of transportable RNAs, if they can be perceived and processed by DCL2 or a DCL2-dependent pathway in recipient cells, could function as systemic silencing signals (Fig. 10A). On the other hand, *DCL4* and *DCL3* could affect *DCL2*-mediated systemic PTGS through their negative regulation of *DCL2* expression (Qin et al., 2017), which would indirectly influence *DCL2* activity in systemic PTGS. Additionally, DCLs may compete with each other for dsRNA substrates. The loss of DCL4 or DCL3 could enhance the DCL2 output, because the level of dsRNA substrate for DCL2 is increased in both incipient and recipient cells. Cross-regulation among *DCLs* could also occur at transcriptional, posttranscriptional, and/or translational levels. These mechanisms may act synergistically for *DCLs* to maximize production of the mobile signals for systemic PTGS (Fig. 10B), in contrast to what has been described in Arabidopsis (Melnyk et al., 2011b; Sarkies and Miska, 2014). Nevertheless, findings from different non-cell autonomous silencing systems may not necessarily be exclusive of each other. There may be various routes to mobile silencing in different plants. *N. benthamiana* is a natural *rdr1* mutant and might behave differently compared to Arabidopsis (Nakasugi et al., 2013). The occurrence of cell-type or tissue dependent functions and specificities of different DCL proteins or different domain arrangements of the DCL proteins has also been reported in *N. benthamiana* (Andika et al., 2015; Nakasugi et al., 2013).

In conclusion, along with our recent work (Qin et al., 2017), we demonstrate that a complex genetic and regulatory network involving *DCL2*, *DCL4*, and *DCL3* may govern the rate and characteristics of the mobile PTGS (Fig. 10). *DCL2* plays a center role in response to mobile signals for systemic PTGS in distal recipient cells. We have also highlighted the potential (non)-involvement of RNAs, including different sized siRNAs, in systemic PTGS. Arabidopsis *DCLs* have distinct functions in mobile silencing, but in *N. benthamiana* their counterparts appear to behave similarly in intracellular silencing to generate miRNAs and 21, 22, or 24 nt siRNAs (this study; Katsarou et al., 2016; Qin et al., 2017), but act coordinately to fulfill different roles in systemic PTGS. Thus, our work provides a new framework to test whether the *DCL2*-centered *DCL* genetic pathway for systemic PTGS is the representative model for the majority of plant species and to unravel mobile signals for systemic PTGS in plants, as well as in (and across) organisms of different kingdoms.

MATERIALS AND METHODS

Plant Materials and Growth Conditions

Non-transformed *Nicotiana benthamiana* and transgenic *N. benthamiana* plants (Table I) were grown and maintained in insect-free glasshouses and growth-rooms at 25°C with supplementary light (13,000 Lux intensity/Visible 40W LED Light Bulbs) to give a 16-h photoperiod.

Plasmid Constructs and Plant Transformation

The GFP_{714} coding sequence (Ryabov et al., 2004) was PCR-amplified and cloned between the duplicated 35S CaMV promoter and the NOS terminator of pJG045, a pCAMBIA1300-based vector, to produce p35S-GFP_{714} (Supplemental

Fig. S1A). To generate gene-specific hairpin *DCL*- and GFP_{714}-RNAi constructs (Supplemental Fig. S1B), cDNA fragments corresponding to nucleotides 4835 to 5075 of *DCL1* (GenBank no. FM986780), nucleotides 3382 to 3582 of *DCL2* (GenBank no. FM986781), nucleotides 4167 to 4347 of *DCL3* (GenBank no. FM986782), nucleotides 3283 to 3482 of *DCL4* (GenBank no. FM986783), or the full-length GFP_{714} (nucleotides 1–714) sequence were cloned into the RNAi vector pRNAi-LIC as described (Xu et al., 2010). There is no sequence similarity among the *DCL* fragments (Supplemental Table S1; Supplemental Data Set S1). The full-length GFP_{714} sequence (Ryabov et al., 2004) was also cloned into pMD18-T (Takara) to produce pT7.GFP from which GFP_{714} RNA transcripts were produced by in vitro transcription using the T7 RNA polymerase. Primers used for these constructs are listed in Supplemental Table S5. All constructs were confirmed by DNA sequencing.

pRNAi-DCL1, pRNAi-DCL2, pRNAi-DCL3, and pRNAi-DCL4 were transformed into the *Agrobacterium tumefaciens* LBA4404, and pRNAi-GFP_{714} and p35S-GFP_{714} were introduced into *A. tumefaciens* EHA105. Transgenic *N. benthamiana* plants were generated by *Agrobacterium*-mediated leaf disc transformation as described (Hong et al., 1996). Two independent homozygous lines (*DCL2Ai* and *DCL2Bi*, *DCL3Ai* and *DCL3Bi*, *DCL4Ai* and *DCL4Bi*) with a single copy of each RNAi construct were obtained. Line *DCL4Bi* was crossed with *DCL2Ai* to produce *DCL24i*. *DCLi* lines were crossed with the GFP transgenic line *16cGFP* that constitutively expresses GFP_{792} (Haseloff et al., 1997; Ruiz et al., 1998) to produce *GfpDCL2Ai*, *GfpDCL2Bi*, *GfpDCL3Ai*, *GfpDCL3B*, *GfpDCL4Ai*, *GfpDCL4Bi*, *GfpDCL24Ai*, and *GfpDCL24Bi*, respectively. At the later stage of this project, we also generated homozygous *homGfpDCL2Ai*, *homGfpDCL3Bi*, *homGfpDCL4Ai*, and *GfpDCL24Ci* through selfing. Only one hemizygous *DCL1i* or *GfpDCL1i* line was generated through direct transformation of *N. benthamiana* or *16cGFP* with pRNAi-DCL1 (Supplemental Fig. S1B). All transgenic lines used in this study are summarized in Table I. It should be noted that *DCL* RNAi is gene-specific and has no obvious off-target effect on other *DCL* and RNA silencing-associated genes (Supplemental Data Set S1; Supplemental Fig. S5 and S10).

Local RNA Silencing and Small RNA Mobility Assay

The experimental design for local RNA silencing and small RNA mobility assay to detect long-distance movement of siRNAs from local to systemic young leaves is outlined in Supplemental Figure S3A. Two young leaves per *N. benthamiana* or *DCLi* plant (six plants at the six-leaf stage in each experiment) were co-infiltrated with 1 OD_{600} agrobacterium harboring p35S-GFP_{714} and agrobacterium harboring pRNAi-GFP_{714} in repeated experiments. In co-infiltrated leaf cells, pRNAi-GFP_{714} is expected to generate hairpin GFP_{714} dsRNA that are diced into siRNAs. These siRNAs targeted and degraded GFP_{714} mRNA transcribed from the p35S-GFP_{714} expression cassette, leading to disappearance of GFP fluorescence. Green fluorescence intensity was measured using ImageJ software following the software provider's guidance (https://imagej.nih.gov/ij/). Infiltrated leaf tissues from three to four different plants at 7 d post agroinfiltration (dpa), and 4 newly developed young leaves of each of 3 to 4 different plants at 14 dpa were collected and pooled for sRNA extraction and construction of sRNA libraries.

Systemic RNA Silencing and Grafting Experiments

Systemic RNA silencing was performed for each line as outlined in Supplemental Figure S9A. Briefly, leaves from six seedlings at the six-leaf stage of transgenic GFP_{792} line *Gfp* and *GfpDCL* RNAi lines were agroinfiltrated with freshly cultured agrobacterium (1 OD_{600}) carrying pRNAi-GFP_{714} as previously described (Hong et al., 2003). Plant grafting was performed as described by Schwach et al. (2005). Induction and spread of *GFP* silencing was routinely examined under long-wavelength UV light and recorded photographically using a Nikon Digital Camera D7000. Red halos on the infiltrated leaves and regions of leaf lamina where *GFP* silencing occurred show red chlorophyll fluorescence, while tissues expressing *GFP* show green fluorescence under long-wavelength UV light. Local and systemic RNA silencing assays were performed for each line in at least two separate experiments. *N. benthamiana* is an allotetraploid (Nakasugi et al., 2014); however, the specific RNAi constructs described above only knock down specific *DCL* expression in spite of the homeologous and duplicated gene copies in the genome. This should not interfere with the analysis of the impact of *DCL* RNAi on cell and noncell autonomous RNA silencing. Agroinfiltrated leaf tissues were collected from 3 to 4 plants at 7 dpa and pooled for sRNA extraction and construction of local sRNA libraries. Young leaves with systemic GFP_{792} PTGS from 3 to 4 plants of each of the *Gfp*, *GfpDCL1i*, *GfpDCL3Bi*, and *GfpDCL4Ai* lines, leaves with weak vein-restricted systemic PTGS from 3 to 4 plants of each of the *GfpDCL2Ai* and *GfpDCL24Ai* lines, or young leaves without systemic PTGS from 3 to 4 plants of each of the *GfpDCL2Ai* and *GfpDCL24Ai* lines were collected at 14 dpa and pooled for sRNA extraction and construction of systemic sRNA libraries.

RNA Extraction and Northern Detection of mRNA and siRNA

For RT-PCR and quantitative real-time PCR (RT-qPCR), total RNAs were extracted from leaf tissues using the RNAprep Pure Plant Kit as recommended by the manufacturer (Tiangen). For northern blot, total RNAs were extracted from leaf tissues with TRIzol reagent as recommended by the manufacturer (Invitrogen). RNAs (5 μg) extracted from infiltrated tissues were separated on a 1% formaldehyde agarose gel, transferred to Hybond-N+ membranes (Amersham Biosciences) by upward capillary transfer in 20× SSC buffer, then cross-linked to the membrane with an UVP CX 2000 UV crosslinker four times (upside, downside, upside, downside) at 120 mJ/cm^2, 1 min each. Membranes were hybridized with digoxigenin-labeled GFP DNA probes prepared using the DIG High Prime DNA Labeling Kit (Roche). RNAs were detected using a DIG Nucleic Acid Detection Kit (Roche) as recommended by the manufacturer. Chemilluminescent signals were detected with a ChemiDoc XRS+ imaging System (Bio-Rad).

To analyze siRNAs, low-molecular-mass sRNAs were enriched from total RNA as described (Hamilton and Baulcombe, 1999). The enriched sRNAs (2.5 μg) were fractionated on an 18% denaturing polyacrylamide/7 M urea gel in 1 x Tris-borate-EDTA buffer. Small RNAs were transferred to Hybond-N+ membranes (Amersham Biosciences) by upward capillary transfer in 20× SSC buffer, then cross-linked to the membranes with an UVP CX 2000 UV Crosslinker four times (upside, underside, upside, underside) at 120 mJ/cm^2, for 1 min each time. The membranes were hybridized with digoxigenin (Dig)-labeled *GFP* RNA probes using a DIG RNA Labeling Kit (Roche) as recommended by the manufacturer. The hybridization chemiluminescence signals were detected with a ChemiDoc XRS+ imaging System (Bio-Rad).

RT-PCR and RT-qPCR

First-strand cDNA was synthesized using 1 μg total RNAs that were pretreated with 1 unit RNase-free DNase I as templates by the M-MLV Reverse Transcriptase (Promega). RT-PCR analyses of GFP_{714} RNA were performed using various sets of primers listed in Supplemental Table S5. The RT-qPCR analyses of *DCL* mRNA levels were performed using *DCL*-specific primers (Supplemental Table S5) and the SYBR Green Mix. The amplification program for SYBR Green I was performed at 95°C for 10 s, 58°C for 30 s, and 72°C for 20 s on a CFX96 real-time PCR detection system (Bio-Rad) following the manufacturer's instructions. Quadruplicate quantitative assays were performed on cDNA of each of the four biological duplicates (leaf tissues from four different treated plants). The relative quantification of *DCL* mRNA was calculated using the Equation $2^{-\Delta\Delta Ct}$ and normalized to the amount of *GAPDH* transcripts (GenBank accession no. TC17509) as described (Qin et al., 2012). RT-qPCR data between control and various treatments were analyzed by Student's *t* test (http://www.physics.csbsju.edu/stats/t-test.html). The statistical significance threshold was $P \leq 0.05$.

Construction of sRNA Library and sRNA NGS

Fragments of 18- to 30-bases-long RNA were isolated from total RNA extracted from pooled samples of three to four different plants for each of the biological and technical duplicates after being separated through 15% denaturing PAGE. The pooled samples contained leaf tissues from three to six leaves per plant. Then sRNAs were excised from the gel and sequentially ligated to a 3′ adapter and a 5′ adapter. After each ligation step, sRNAs were purified after 15% denaturing PAGE. The final purified ligation products were reverse-transcribed into cDNA using reverse transcriptase (Finnzymes Oy). The first-strand cDNA was PCR amplified using Phusion* DNA Polymerase (Finnzymes Oy). The purified DNA fragments were used for clustering and sequencing by Illumina HisEquation 2000 (Illumina) at the Beijing Genomics Institute.

Bioinformatics Analysis of sRNA Sequences

Illumina HighSEquation 2000 sequencing produced a similar number of 11 to 12 million reads per sRNA library. The reads were cropped to remove adapter sequences and were aligned to the reference sequences using Bowtie2

(Langmead and Salzberg, 2012). Reference sequences include hairpin GFP_{714} (Ryabov et al., 2004), GFP_{792} transgene (Haseloff et al., 1997), *DCL1*, *DCL2*, *DCL3*, and *DCL4* gene sequences (Nakasugi et al., 2013) and a set of 50 tobacco miRNAs identified in *Nicotiana* plants (Pandey et al., 2008; Figure 5; Supplemental Data Set S1). SAMtools pileup was used to produce the siRNA and miRNA coverage profiles (Li et al., 2009). For correlation analyses for sRNA libraries, the number of miRNA hits corresponding to the previously identified set of 50 *Nicotiana* miRNAs was determined. All analyzed sRNA libraries for local and systemic leaf samples contained similar proportions of host-encoded miRNA reads (Nakasugi et al., 2013; Ryabov et al., 2014), indicating equivalence and direct comparability of the datasets and no variation due to the efficiency of library preparation and sequencing (Supplemental Tables S2 and S7; Supplemental Figures S5, S6, S10, and S11). Outcomes of comparisons between normalized siRNAs against the total sRNA reads (per 10 million sRNA reads) are consistent with the numbers of siRNA reads directly compared.

Accession Numbers

DCL1: GenBank number FM986780; *DCL2*: GenBank number FM986781; *DCL3*: GenBank number FM986782; *DCL4*: GenBank number FM986783; and *GAPDH*: GenBank accession number TC17509.

Supplemental Data

The following supplemental materials are available.

Supplemental Table S1. Nucleotide sequence similarity (%) between *DCL* fragments in the pRNAi-DCLs constructs.

Supplemental Table S2. Summary of sRNAseq datasets of 18 GFP_{714} sRNA libraries for long-distance spread of siRNAs.

Supplemental Table S3. Correlation analyses of miRNA profiles among agro-infiltrated leaf sRNA libraries (Nb background).

Supplemental Table S4. Correlation analyses of miRNA profiles among systemic leaf sRNA libraries (Nb background).

Supplemental Table S5. Primers used in this study.

Supplemental Table S6. Impact of *DCL* RNAi on systemic PTGS.

Supplemental Table S7. Summary of sRNAseq datasets of 14 sRNA libraries for local and systemic PTGS.

Supplemental Table S8. Correlation analyses of miRNA profiles among agro-infiltrated leaf sRNA libraries (16cGFP transgenic background).

Supplemental Table S9. Correlation analyses of miRNA profiles among systemic leaf sRNA libraries (16cGFP transgenic background).

Supplemental Figure S1. Construction of gene expression and RNAi vectors.

Supplemental Figure S2. RNAi effects on *DCL* gene expression.

Supplemental Figure S3. NGS detection of total small RNAs in local and systemic leaves.

Supplemental Figure S4. Effect of *DCL* RNAi on local GFP_{714} RNA silencing.

Supplemental Figure S5. *DCL* RNAi does not cause off-target silencing of genes associated with RNAi pathways in Nb background plants: sRNA reads in 18 sRNA libraries.

Supplemental Figure S6. miRNA reads in 18 sRNA libraries (Nb background).

Supplemental Figure S7. No long-distance movement of large GFP_{714} RNA.

Supplemental Figure S8. Impact of *DCL* RNAi on systemic PTGS.

Supplemental Figure S9. Size profiles for total sRNAs in local and systemic leaves.

Supplemental Figure S10. *DCL* RNAi does not cause off-target silencing of genes associated with RNAi pathways in 16cGFP transgenic background plants: sRNA reads in 14 sRNA libraries.

Supplemental Figure S11. miRNA reads in 14 sRNA libraries (16cGFP transgenic background).

Supplemental Figure S12. Specific 21-24nt siRNA distributions across the transgene GFP_{792} mRNA.

Supplemental Data Set S1. Reference sequences used in this study.

Supplemental Data Set S2. *DCL* RNAi does not cause off-target silencing of genes associated with RNAi pathways in Nb backgound plants: sRNA reads in 18 sRNA libraries.

Supplemental Data Set S3. miRNA reads in 18 sRNA libraries (Nb background).

Supplemental Data Set S4. *DCL* RNAi does not cause off-target silencing of genes associated with RNAi pathways in 16cGFP transgenic background plants: sRNA reads in 14 sRNA libraries.

Supplemental Data Set S5. miRNA reads in 14 sRNA libraries (16cGFP transgenic background).

ACKNOWLEDGMENTS

We are indebted to David Baulcombe for his kind gift of *16cGFP*, *RDR6i*, and *GfpRDR6i* seeds and for his constructive and critical comments on the manuscript. The corresponding author thanks Mahmut Tör for reading the manuscript. No conflict of interest is declared.

Received January 2, 2018; accepted January 25, 2018; published February 8, 2018.

LITERATURE CITED

Andika IB, Maruyama K, Sun L, Kondo H, Tamada T, Suzuki N (2015) Differential contributions of plant Dicer-like proteins to antiviral defences against potato virus X in leaves and roots. Plant J **81:** 781–793

Baulcombe D (2004) RNA silencing in plants. Nature **431:** 356–363

Berg JM (2016) Retraction. Science **354:** 190

Bouché N, Lauressergues D, Gasciolli V, Vaucheret H (2006) An antagonistic function for Arabidopsis DCL2 in development and a new function for DCL4 in generating viral siRNAs. EMBO J **25:** 3347–3356

Brosnan CA, Mitter N, Christie M, Smith NA, Waterhouse PM, Carroll BJ (2007) Nuclear gene silencing directs reception of long-distance mRNA silencing in Arabidopsis. Proc Natl Acad Sci USA **104:** 14741–14746

Carlsbecker A, Lee JY, Roberts CJ, Dettmer J, Lehesranta S, Zhou J, Lindgren O, Moreno-Risueno MA, Vatén A, Thitamadee S, et al (2010) Cell signalling by microRNA165/6 directs gene dose-dependent root cell fate. Nature **465:** 316–321

Chen HM, Chen LT, Patel K, Li YH, Baulcombe DC, Wu SH (2010) 22-Nucleotide RNAs trigger secondary siRNA biogenesis in plants. Proc Natl Acad Sci USA **107:** 15269–15274

Cuperus JT, Carbonell A, Fahlgren N, Garcia-Ruiz H, Burke RT, Takeda A, Sullivan CM, Gilbert SD, Montgomery TA, Carrington JC (2010) Unique functionality of 22-nt miRNAs in triggering RDR6-dependent siRNA biogenesis from target transcripts in Arabidopsis. Nat Struct Mol Biol **17:** 997–1003

Devanapally S, Ravikumar S, Jose AM (2015) Double-stranded RNA made in C. elegans neurons can enter the germline and cause transgenerational gene silencing. Proc Natl Acad Sci USA **112:** 2133–2138

Dunoyer P, Himber C, Voinnet O (2005) DICER-LIKE 4 is required for RNA interference and produces the 21-nucleotide small interfering RNA component of the plant cell-to-cell silencing signal. Nat Genet **37:** 1356–1360

Feinberg EH, Hunter CP (2003) Transport of dsRNA into cells by the transmembrane protein SID-1. Science **301:** 1545–1547

Garcia-Ruiz H, Takeda A, Chapman EJ, Sullivan CM, Fahlgren N, Brempelis KJ, Carrington JC (2010) Arabidopsis RNA-dependent RNA polymerases and dicer-like proteins in antiviral defense and small interfering RNA biogenesis during Turnip Mosaic Virus infection. Plant Cell **22:** 481–496

Hamilton AJ, Baulcombe DC (1999) A species of small antisense RNA in posttranscriptional gene silencing in plants. Science **286:** 950–952

Haseloff J, Siemering KR, Prasher DC, Hodge S (1997) Removal of a cryptic intron and subcellular localization of green fluorescent protein are required to mark transgenic Arabidopsis plants brightly. Proc Natl Acad Sci USA **94:** 2122–2127

Henderson IR, Zhang X, Lu C, Johnson L, Meyers BC, Green PJ, Jacobsen SE (2006) Dissecting Arabidopsis thaliana DICER function in small RNA processing, gene silencing and DNA methylation patterning. Nat Genet **38:** 721–725

Hong Y, Saunders K, Hartley MR, Stanley J (1996) Resistance to geminivirus infection by virus-induced expression of dianthin in transgenic plants. Virology **220:** 119–127

Hong Y, Stanley J, van Wezel R (2003) Novel system for the simultaneous analysis of geminivirus DNA replication and plant interactions in Nicotiana benthamiana. J Virol **77:** 13315–13322

Jose AM, Garcia GA, Hunter CP (2011) Two classes of silencing RNAs move between *Caenorhabditis elegans* tissues. Nat Struct Mol Biol **18:** 1184–1188

Jose AM, Smith JJ, Hunter CP (2009) Export of RNA silencing from C. elegans tissues does not require the RNA channel SID-1. Proc Natl Acad Sci USA **106:** 2283–2288

Katsarou K, Mavrothalassiti E, Dermauw W, Van Leeuwen T, Kalantidis K (2016) Combined activity of DCL2 and DCL3 is crucial in the defense against potato spindle tuber viroid. PLoS Pathog **12:** e1005936

Langmead B, Salzberg SL (2012) Fast gapped-read alignment with Bowtie 2. Nat Methods **9:** 357–359

Lewsey MG, Hardcastle TJ, Melnyk CW, Molnar A, Valli A, Urich MA, Nery JR, Baulcombe DC, Ecker JR (2016) Mobile small RNAs regulate genome-wide DNA methylation. Proc Natl Acad Sci USA **113:** E801–E810

Li H, Handsaker B, Wysoker A, Fennell T, Ruan J, Homer N, Marth G, Abecasis G, Durbin R; 1000 Genome Project Data Processing Subgroup (2009) The sequence alignment/map format and SAMtools. Bioinformatics **25:** 2078–2079

Mallory AC, Ely L, Smith TH, Marathe R, Anandalakshmi R, Fagard M, Vaucheret H, Pruss G, Bowman L, Vance VB (2001) HC-Pro suppression of transgene silencing eliminates the small RNAs but not transgene methylation or the mobile signal. Plant Cell **13:** 571–583

Melnyk CW, Molnar A, Bassett A, Baulcombe DC (2011a) Mobile 24 nt small RNAs direct transcriptional gene silencing in the root meristems of *Arabidopsis thaliana*. Curr Biol **21:** 1678–1683

Melnyk CW, Molnar A, Baulcombe DC (2011b) Intercellular and systemic movement of RNA silencing signals. EMBO J **30:** 3553–3563

Mlotshwa S, Pruss GJ, Peragine A, Endres MW, Li J, Chen X, Poethig RS, Bowman LH, Vance V (2008) DICER-LIKE2 plays a primary role in transitive silencing of transgenes in Arabidopsis. PLoS One **3:** e1755

Molnar A, Melnyk CW, Bassett A, Hardcastle TJ, Dunn R, Baulcombe DC (2010) Small silencing RNAs in plants are mobile and direct epigenetic modification in recipient cells. Science **328:** 872–875

Mukherjee K, Campos H, Kolaczkowski B (2013) Evolution of animal and plant dicers: early parallel duplications and recurrent adaptation of antiviral RNA binding in plants. Mol Biol Evol **30:** 627–641

Nakasugi K, Crowhurst R, Bally J, Waterhouse P (2014) Combining transcriptome assemblies from multiple de novo assemblers in the allotetraploid plant Nicotiana benthamiana. PLoS One **9:** e91776

Nakasugi K, Crowhurst RN, Bally J, Wood CC, Hellens RP, Waterhouse PM (2013) *De novo* transcriptome sequence assembly and analysis of RNA silencing genes of *Nicotiana benthamiana*. PLoS One **8:** e59534

Pandey SP, Shahi P, Gase K, Baldwin IT (2008) Herbivory-induced changes in the small-RNA transcriptome and phytohormone signaling in Nicotiana attenuata. Proc Natl Acad Sci USA **105:** 4559–4564

Pant BD, Buhtz A, Kehr J, Scheible W-R (2008) MicroRNA399 is a long-distance signal for the regulation of plant phosphate homeostasis. Plant J **53:** 731–738

Parent J-S, Bouteiller N, Elmayan T, Vaucheret H (2015) Respective contributions of Arabidopsis DCL2 and DCL4 to RNA silencing. Plant J **81:** 223–232

Qin C, Li B, Fan Y, Zhang X, Yu Z, Ryabov E, Zhao M, Wang H, Shi N, Zhang P, et al (2017) Roles of DCL2 and DCL4 in Intra- and Intercellular Antiviral Silencing in *Nicotiana benthmiana*. Plant Physiol **174:** 1067–1081

Qin C, Shi N, Gu M, Zhang H, Li B, Shen J, Mohammed A, Ryabov E, Li C, Wang H, et al (2012) Involvement of RDR6 in short-range intercellular RNA silencing in Nicotiana benthamiana. Sci Rep **2:** 467

Qu F, Ye X, Morris TJ (2008) Arabidopsis DRB4, AGO1, AGO7, and RDR6 participate in a DCL4-initiated antiviral RNA silencing pathway negatively regulated by DCL1. Proc Natl Acad Sci USA **105:** 14732–14737

Ruiz MT, Voinnet O, Baulcombe DC (1998) Initiation and maintenance of virus-induced gene silencing. Plant Cell **10:** 937–946

Ryabov EV, van Wezel R, Walsh J, Hong Y (2004) Cell-to-cell, but not long-distance, spread of RNA silencing that is induced in individual epidermal cells. J Virol **78:** 3149–3154

Ryabov EV, Wood GR, Fannon JM, Moore JD, Bull JC, Chandler D, Mead A, Burroughs N, Evans DJ (2014) A virulent strain of *deformed wing virus* (DWV) of honeybees (*Apis mellifera*) prevails after Varroa destructor-mediated, or in vitro, transmission. PLoS Pathog **10:** e1004230

Sarkies P, Miska EA (2014) Small RNAs break out: the molecular cell biology of mobile small RNAs. Nat Rev Mol Cell Biol **15:** 525–535

Searle IR, Pontes O, Melnyk CW, Smith LM, Baulcombe DC (2010) JMJ14, a JmjC domain protein, is required for RNA silencing and cell-to-cell movement of an RNA silencing signal in Arabidopsis. Genes Dev **24:** 986–991

Schwach F, Vaistij FE, Jones L, Baulcombe DC (2005) An RNA-dependent RNA polymerase prevents meristem invasion by potato virus X and is required for the activity but not the production of a systemic silencing signal. Plant Physiol **138:** 1842–1852

Shih JD, Hunter CP (2011) SID-1 is a dsRNA-selective dsRNA-gated channel. RNA **17:** 1057–1065

Skopelitis DS, Benkovics AH, Husbands AY, Timmermans MCP (2017) Boundary formation through a direct threshold-based readout of mobile small RNA gradients. Dev Cell **43:** 265–273.e6

Smith LM, Pontes O, Searle I, Yelina N, Yousafzai FK, Herr AJ, Pikaard CS, Baulcombe DC (2007) An SNF2 protein associated with nuclear RNA silencing and the spread of a silencing signal between cells in Arabidopsis. Plant Cell **19:** 1507–1521

Taochy C, Gursanscky NR, Cao J, Fletcher SJ, Dressel U, Mitter N, Tucker MR, Koltunow AMG, Bowman JL, Vaucheret H, et al (2017) A genetic screen for impaired systemic RNAi highlights the crucial role of DICER-LIKE 2. Plant Physiol **175:** 1424–1437

Wang XB, Jovel J, Udomporn P, Wang Y, Wu Q, Li WX, Gasciolli V, Vaucheret H, Ding SW (2011) The 21-nucleotide, but not 22-nucleotide, viral secondary small interfering RNAs direct potent antiviral defense by two cooperative argonautes in Arabidopsis thaliana. Plant Cell **23:** 1625–1638

Weiberg A, Wang M, Lin FM, Zhao H, Zhang Z, Kaloshian I, Huang HD, Jin H (2013) Fungal small RNAs suppress plant immunity by hijacking host RNA interference pathways. Science **342:** 118–123

Winston WM, Molodowitch C, Hunter CP (2002) Systemic RNAi in C. elegans requires the putative transmembrane protein SID-1. Science **295:** 2456–2459

Xie Z, Allen E, Wilken A, Carrington JC (2005) DICER-LIKE 4 functions in trans-acting small interfering RNA biogenesis and vegetative phase change in Arabidopsis thaliana. Proc Natl Acad Sci USA **102:** 12984–12989

Xie Z, Johansen LK, Gustafson AM, Kasschau KD, Lellis AD, Zilberman D, Jacobsen SE, Carrington JC (2004) Genetic and functional diversification of small RNA pathways in plants. PLoS Biol **2:** E104

Xu G, Sui N, Tang Y, Xie K, Lai Y, Liu Y (2010) One-step, zero-background ligation-independent cloning intron-containing hairpin RNA constructs for RNAi in plants. New Phytol **187:** 240–250

Yelina NE, Smith LM, Jones AM, Patel K, Kelly KA, Baulcombe DC (2010) Putative Arabidopsis THO/TREX mRNA export complex is involved in transgene and endogenous siRNA biosynthesis. Proc Natl Acad Sci USA **107:** 13948–13953